CLEAN SKY 2

JTI-CS2-2020-CFP11-THT-13: Sustainability of Hybrid-Electric Aircraft System Architectures

GENESIS

GAUGING THE ENVIRONMENTAL SUSTAINABILITY OF ELECTRIC AIRCRAFT SYSTEM

D1.1

Overall Requirements for (hybrid) electric 50 pax regional class A/C

Deliverable No.	GENESIS D1.1
Deliverable Title	Overall Requirements for (hybrid) electric 50 pax regional class A/C
Deliverable Date	31/07/2021
Version	1.0
Deliverable Type	Report
Dissemination level	Public
Link to scientific publication and/or repository	To be provided (paper in preparation)
Written By	Fabrizio Nicolosi (UniNa), Valerio Marciello (UniNa), Francesco Orefice (UniNa), Mario Di Stasio (UniNa), Salvatore Corcione (UniNa), Manuela Ruocco (SmartUp), Vincenzo Cusati (SmartUp)
Checked by	NA
Contact persons	F.N. (fabrnico@unina.it), M.R. (manuela.ruocco@smartup-engineering.com)
Status	Submitted

This project has received funding from the Clean Sky 2 Joint Undertaking (JU) under grant agreement No 101007968. The JU receives support from the European Union's Horizon 2020 research and innovation programme and the Clean Sky 2 JU members other than the Union. This deliverable only reflects the author's view; the JU is not responsible for any use that may be made of the information it contains.

About project GENESIS

In a global context, where modern societies need to move towards more environmental sustainability, the aviation sector has an important role to play. Transition to reduce its environmental footprint (i.e. impacts on ecosystems, human health and natural resources) stemming from activities in the entire value chain of aircraft, has become high on political and industrial agenda. This transition must go hand in hand with the technological transformation of aircraft systems, moving away from the use of fossil-based fuels to alternative energy sources, like biofuels, hydrogen or electricity via batteries.

Project GENESIS, funded by the EU Commission under the Clean Sky 2 Programme, aims to tackle some of these challenges. GENESIS stands for "Gauging the environmental sustainability of electric and hybrid aircraft". Its main purpose is to develop a technology and sustainability roadmap to support the ambitions of the European aviation industry for transitioning towards environmentally sustainable and competitive electric and hybrid aircraft systems. Several powertrain technology alternatives are explored, including conventional, batteries, fuel cells and hybrid combinations of them, all with three time perspectives over the period 2020-2050.

Organized around a multidisciplinary and complementary expertise of its consortium members, GENESIS has the following key objectives (each reflecting the WP1-3 structure of GENESIS):

1. Develop a conceptual design, associated with top level aircraft requirements and scenarios, for all-electric and hybrid 50 PAX regional class aircraft.
2. Perform technology foresight analyses on key elements of the aircraft system, focusing on the powertrain architecture and energy storage alternatives.
3. Build life cycle inventories for each relevant technology processes within the aircraft life cycle (from resource extraction, through manufacturing and use, up to end-of-life), and use them to perform prospective life cycle assessment of future aircraft system configurations and scenarios.

Overview and role of this deliverable within GENESIS project

This document describes the initial Top Level Aircraft Requirements (TLARs) regarding the new regional aircraft 50 pax class and defines key specifications in terms of powertrain and energy storage system. The output of this deliverable represents a starting point for further analysis in WP2 end plays a key role in the design iterative process. Define an initial set of TLARs and the powertrain configuration helps to finalize the new advanced A/C design toolchain capable of designing reliable hybrid/all-electric aircraft system to overcome existing technical barriers for electrical energy storage, transmission, and supply, and to integrate a systemic and life cycle perspective in its coverage of emerging energy storage and propulsive system technologies to operate the transition towards eco-design driven electric aircraft solutions (SO-1, SO-2 of GENESIS project). Moreover, the market scenario analysis helps to define future aircraft requirement in the same segment.

Table of contents

List of figures and tables

Executive Summary

Purpose of this document is to define the Top-Level Aircraft Requirements (TLAR) for a 50 pax regional class hybrid/electric aircraft and to identify key specifications in terms of on-board energy storage, shaft power level and weight.

The starting point is a scenario analysis of the aircraft segment that led to increased awareness of the need to design more environmentally sustainable aircraft. The definition of TLARs is done by performing a detailed study of the most relevant regional aircraft both turboprop and jet engine. The overall key factor that guides the definition of TLARs for GENESIS (Gauging the ENvironmEntal Sustainability of electrIc aircraft Systems) is to make economically attractive the new 50-pax regional aircraft paying attention on current and future routes.

Sec. 1 describes the drivers of the definition of a new regional aircraft focusing on the environmental impact of conventional ones defined by SMARTUP. In Sec. 2 a deep market analysis is done to define benchmark aircraft used for the derivation of GENESIS TLARs. The paragraph 2.3 is dedicated to COVID-19 effect on the aviation. Finally in Sec. 3, the initial set of TLARs is defined.

After presenting the general requirements, Sec. 4 introduces an approach for the design and the integration of hybrid-electric propulsion architectures within the aircraft design chain developed by UNINA. First, a general scheme of hybrid-electric powerplant is described and it is explained how to derive a multitude of specific architectures from it, depending on the degree of hybridization or the number and type of energy sources and electrical units. Several preliminary technological levels for batteries are proposed for the different time horizons. Paragraphs 4.3, 4.4 and 4.5 introduce mathematical models for the description of the aero-propulsive effects, essential to fully capture the advantages of hybridization since the first stages of the design process. Based on these, distributed electric propulsion has been identified as the most promising innovative technology. In particular, a configuration with 2 thermal engines, 8 distributed electric motors and a battery group was chosen for the initial assessment of the mission energy requirement, presented in Sec. 5. The reference powers of the individual propulsive elements, as well as the estimated hydrogen masses for hybridization based on hydrogen fuel cells, are finally extrapolated.

1. Time for a new design aircraft

1.1. Analysis of aircraft market emissions

Mobility and transports are of primary importance to the entire global economy and society. Transports underpin social connections and facilitate access to goods and services, and they are moved forward to a more efficiency, more speed and accessibility even if this raises the issue about sustainability. As matter of fact, global emissions from transports have increased a lot over the past half-century. However, 74.5% of transport emissions came from road vehicles and the global aviation industry produces around 2% of all human-induced carbon dioxide (CO2) emissions, and it is responsible for 12% of CO_2 emission of all transports sources. Besides these data, the airline passenger efficiency is satisfying with an average occupancy of aircraft of 82%, definitely greater than other forms of transport (ATAG Air Transport Action Group, 2021) as shown in Figure 1. Aviation, therefore, turns out to be one of the most efficient, safest and most reliable modes of transportation in the world today but, despite this, aviation emissions need to be reduced to comply the key objectives mentioned in EUROPE2020 and in Flightpath2050. Innovation in technology and approaches today facing the environmental expectations and the growth of demands. In fact, the aviation sector is growing fast and will continue to grow. The most recent estimates suggest that demand for air transport will increase by an average of 4.3% per annum over the next 20 years.

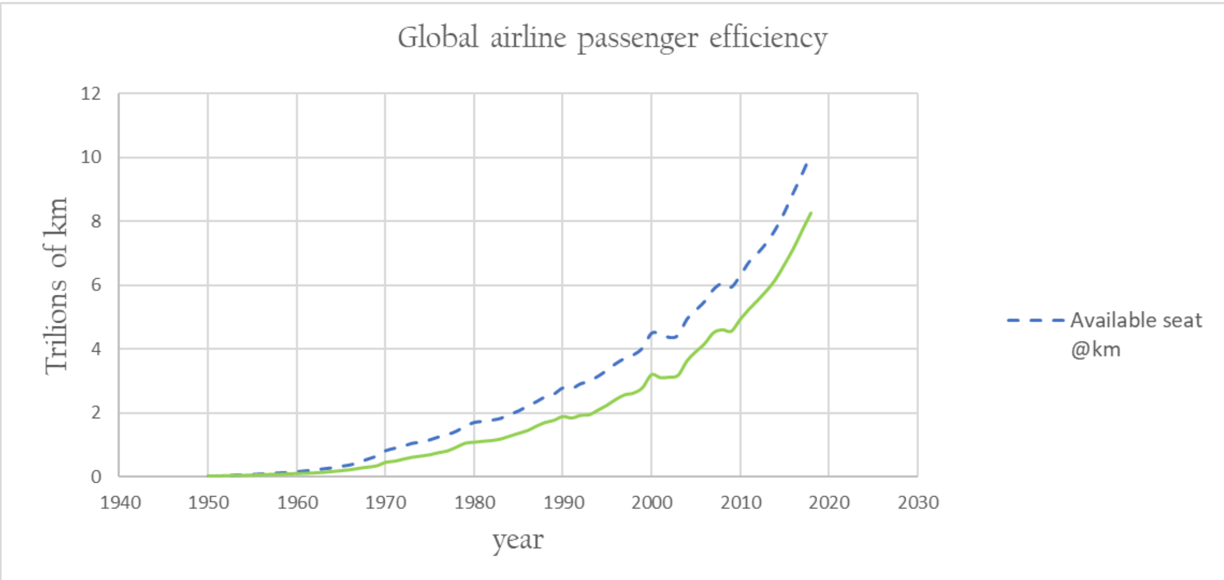

Figure 1. Global airline passenger efficiency.

The carbon dioxide emissions released by global fossil fuel combustion and industrial processes have seen a dramatic rise since the birth of the industrial revolution. Since 1950, aviation emissions increased almost seven-fold, since 1960 they have tripled. Air traffic volume – here defined as revenue passenger kilometers (RPK) traveled – increased by orders of magnitude more: almost 300-fold since 1950; and 75-fold since 1960. Most recently, in 2019, the world saw roughly 36.44 billion metric tons of carbon dioxide emitted. Despite the fact that the 2020 shows a noticeable reduction in emissions due to the impacts of COVID-19, it will increase again (Figure 2). From 2013 to 2018, carbon dioxide (CO_2) emissions from commercial aviation increased about 70% faster than United Nations projections (Graver, Zhang, & Rutherford, 2019), and they were recently on track to triple by 2050, which means they could account for one-quarter of CO_2 emissions from all sectors by then.

Transport accounts for around one-fifth of global carbon dioxide (CO_2) emissions. Road travel accounts for three-quarters of transport emissions. Most of this comes from passenger vehicles – cars and buses – which contribute 45.1%. The other 29.4% comes from trucks carrying freight.

Since the entire transport sector accounts for 21% of total emissions, road transport accounts for 15% of total CO2 emissions. Aircraft contribution represented 2.5% of total CO2 emissions in 2018 and 11.6 % of transport (OurWorldinData.org – Research and data to make progress against the world's largest problems, 2021)(Figure 3).

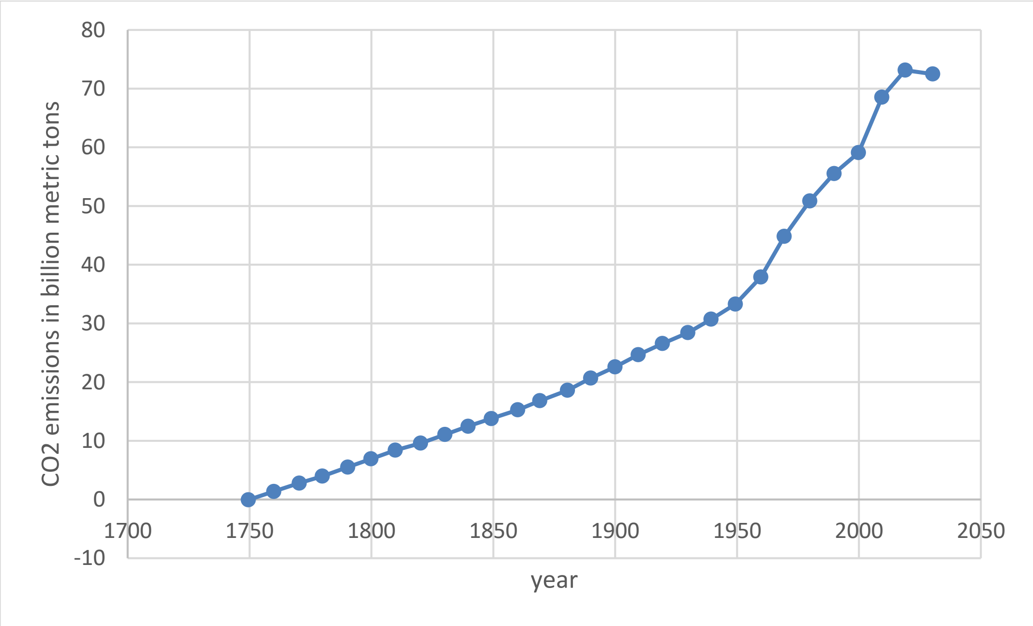

Figure 2. Global historical CO2 emissions 1758-2020. **(Statista.com, 2021)**

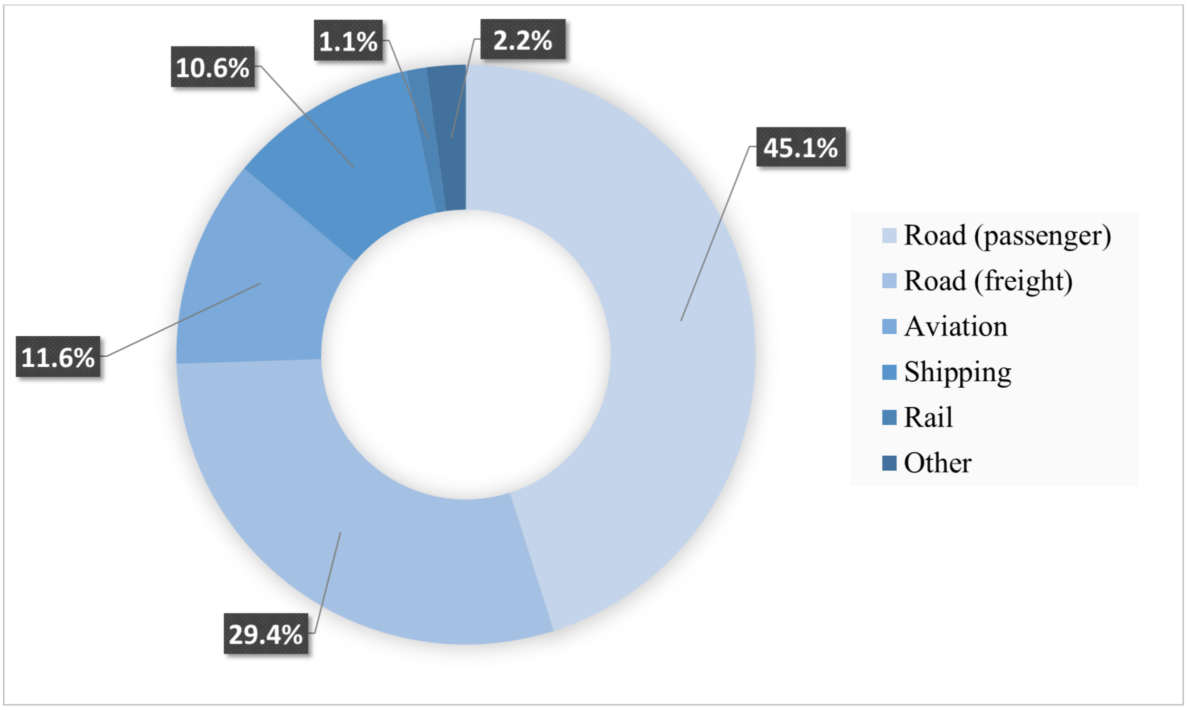

Figure 3. Global CO_2 emissions from transports.

In light of the above current European plans for future aviation involve a major effort in the reduction of both noise and pollutant emissions from airplanes. A radical innovation is required to satisfy the key objectives mentioned in EUROPE2020 and in Flightpath2050.

1.2. Analysis of emissions by segment and aircraft class

In this section SMARTUP aircraft emissions analysis is reported, taking into account different segment and aircraft classes. For air transport purposes, the number of kilometers traveled by paying passengers it is usually measured by the Revenue Passenger Kilometers (RPKs), that is the sum of the products obtained by multiplying the number of revenue passengers carried on each flight stage by the corresponding stage distance.

$$RPKs = \sum P \cdot D[km]$$

Passenger flights are responsible for approximately 85% of commercial aviation CO_2 emissions. In 2019, this amounted to 785 million tonnes (Mt) of CO_2 and this value increased by 33% in the previous 6 years. Over the same period, the number of flight departures increased 22% and revenue passenger kilometers (RPKs) increased 50%. This means that passenger air traffic increased nearly four times faster than fuel efficiency improved.

It is possible to estimate CO_2 emissions taking into account the aircraft class. Data are referred to 2019 due to the COVID-19 impact on air traffic. More than 60% of all passenger flights were operated on narrowbody aircraft in 2019, and these accounted for more than half of all RPKs and passenger CO_2 emissions. On average, global passenger aircraft emitted 90 g CO_2 per kilometer in 2019. That is 2% lower than in 2018, and 12% lower than in 2013. However, smaller regional aircraft that are used on shorter flights emitted nearly 80% more CO_2 per kilometer than the global average for all aircraft (ICCT - The International Council of Clean Transportation, 2020), Figure 4.

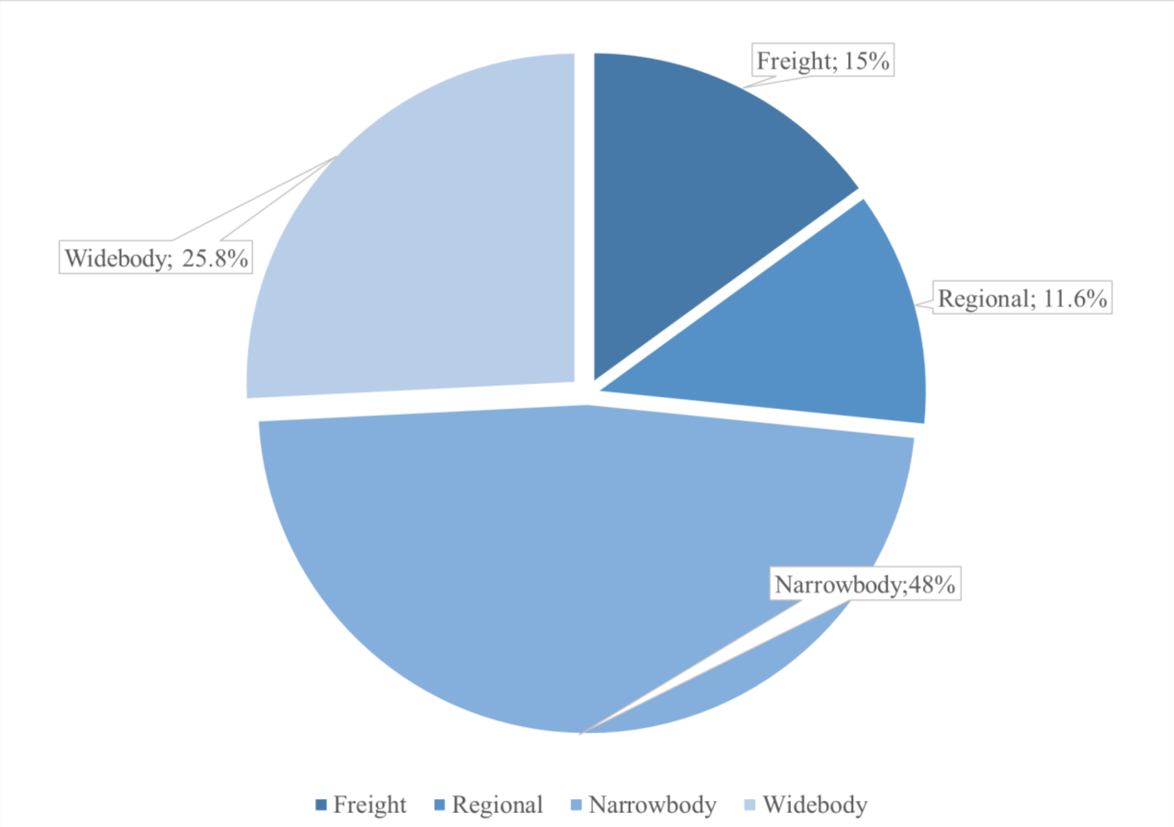

Figure 4. Global CO2 emissions in Mt for aircraft class in 2019.

Moreover, is it possible to underline the emission contributions of different classes. Premium class seats take up a larger footprint compared with economy one: with fewer passengers on each flight and larger footprints, the emissions credited to premium passengers per kilometer are greater than for economy passengers.

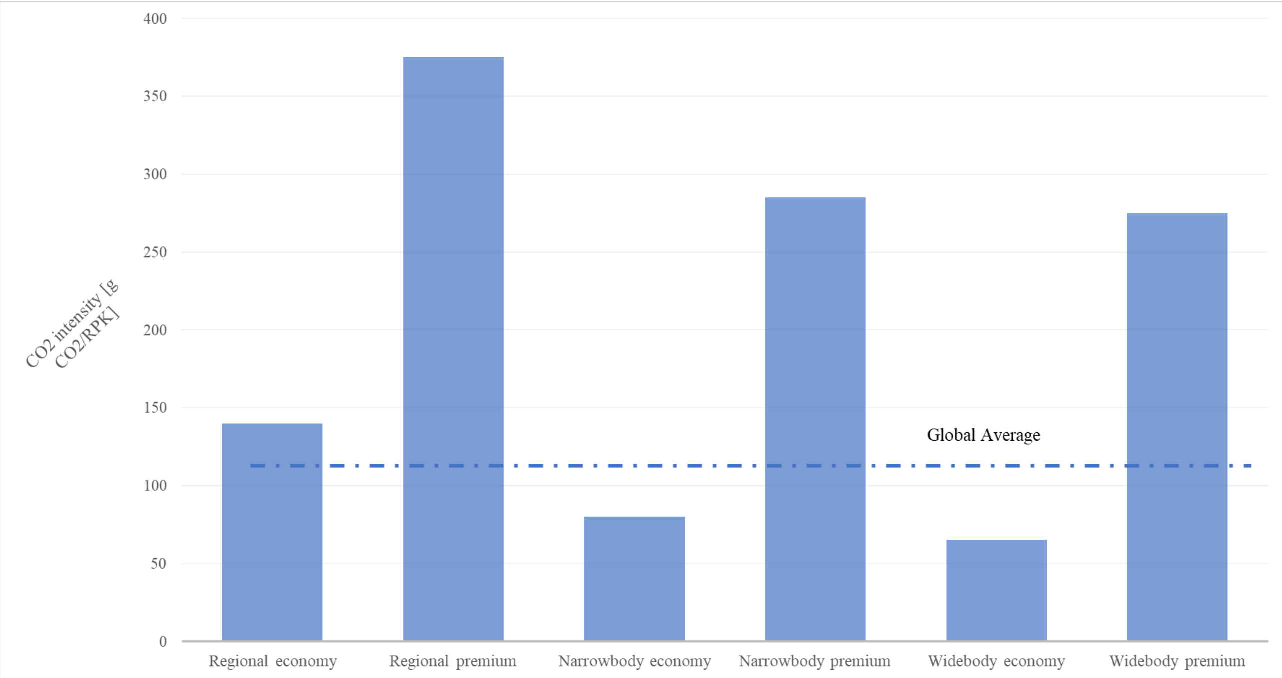

Figure 5. CO2 emissions intensity by aircraft class and segment.

As shown in Figure 5, considering the CO_2 intensity emission, evaluated with respect to RPKs, the regional segment aircraft is greater than the global average of 90 g CO_2 /km.

On average, narrowbodies and widebodies had similar carbon intensity, but regional aircraft CO_2 emissions intensity is definitely higher than other classes (Table 1). Another aspect to take into account is the emissions from the top six regional aircraft have all increased in the last decade, while those from the smaller Canadair and Embraer regional jets that round out the top 10 have decreased. The most fuel efficient of the top 10 regional aircraft are both turboprop aircraft: the De Havilland Dash 8-400 and the ATR 72-600 (Table 2), (Figure 6). These two accounted for the most departures by regional aircraft globally with more than 1 million flights each. However, they rank in the middle of the 10 aircraft analyzed because larger regional jets have a higher number of seats and longer flight distances (Graver, Zhang, & Rutherford, 2019).

Table 1: Passenger CO_2 emissions and intensity by aircraft class.

	Departures (% of total)	RPKs billion	RPKs percentage	Average distance [km]	CO2 emissions [Mt]	CO2 intensity [g CO2/RPK]
Regional	29	345	4	551	56	162
Narrowbody	63	4.588	53	1322	393	86
Widebody	8	3.777	43	4675	336	89
Total	100	8.710	100	1378	785	90

Table 2. Passenger CO_2 emissions from the top 10 regional aircraft types in 2013 and 2019.

Aircraft	Average seats	CO_2 emissions [Mt]		Delta percentage
		2013	2019	
Embraer E190	100	8.76	9.54	9%
Embraer E175	77	2.53	6.94	174%
CRJ900	80	3.37	6.4	90%
De Havilland Dash8-400	73	2.84	2.84	3.96
Embraer E195 11	116	2.5	3.51	41%
ATR 72-600	69	2	3.28	64%
Embraer ERJ145	50	6.07	3.04	-50%
CRJ200	50	5.75	2.95	-49%
CRJ700	68	4.07	2.9	-29%
Embraer E170	74	2.68	2.44	-9%

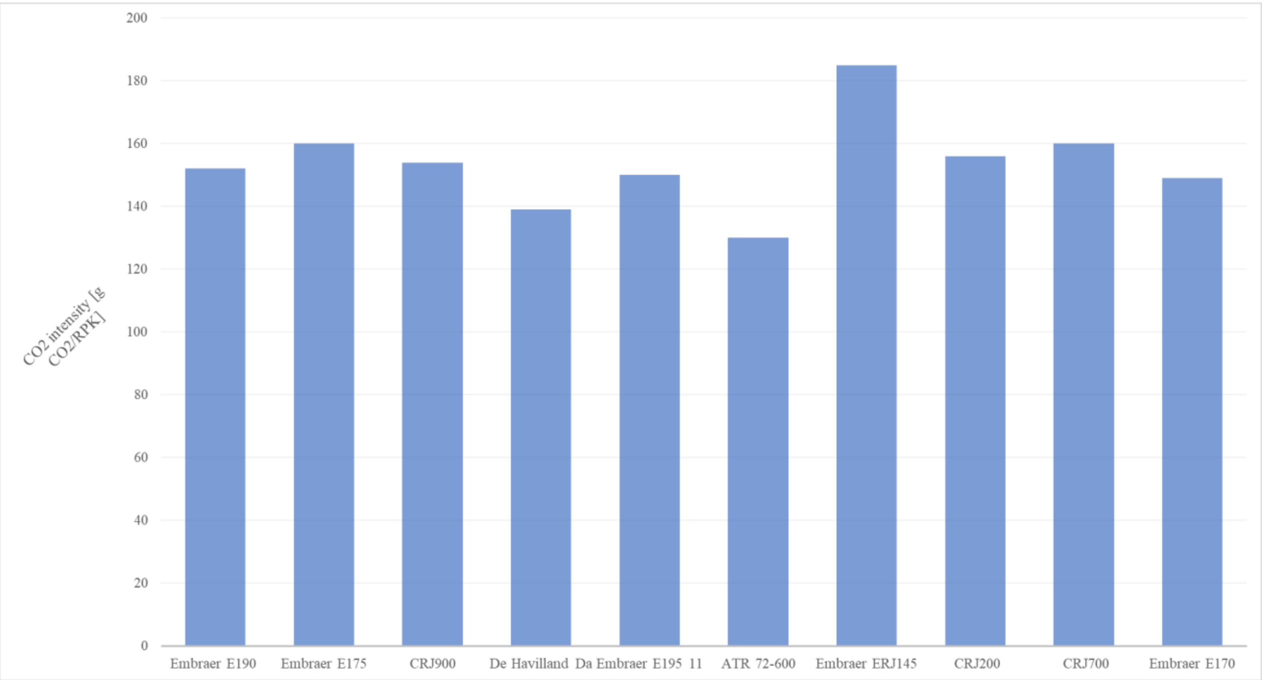

Figure 6. Passenger CO_2 intensity of the 10 highest emitting regional aircraft types.

1.3. Environmental sustainability of future aircraft

The aviation industry is changing fast. Research centers and industries are moving forward new projects aimed at sustainability and emission reduction and this ambitious target cannot be achieved using existing aircraft technologies. Alternative propulsion systems and energy sources, and innovative solutions to existing challenges, will help us to significantly reduce CO_2 emissions in future aircraft. The aviation industry has made sweeping commitments to sustainability by 2050 and there has been immense interest in new sustainability efforts, accounting for factors such as demographic and economic growth, tourism trends, oil prices, development of new and existing routes. In order to accomplish the goal of environmental sustainability of future aircraft, aviation industry is working from aerodynamic design changes to aircraft and engines; use of lighter materials and innovative processes in the manufacture of both airframe and interior components; and the development and use of alternative fuels. One of the ways to significantly reduce CO_2 emissions in a new propulsive system: the hybrid/electric propulsion (Figure 7). The outlook for the development of airplanes with hybrid/electric propulsion is evolving in parallel with the evolution of enabling technologies in the field of electrical systems. Moreover, the adoption of this new technology is bounded to its cost-effectiveness. The transition to hybrid-electric aircraft is subjected to the price of new elements: batteries, power plant, chargers and electricity.

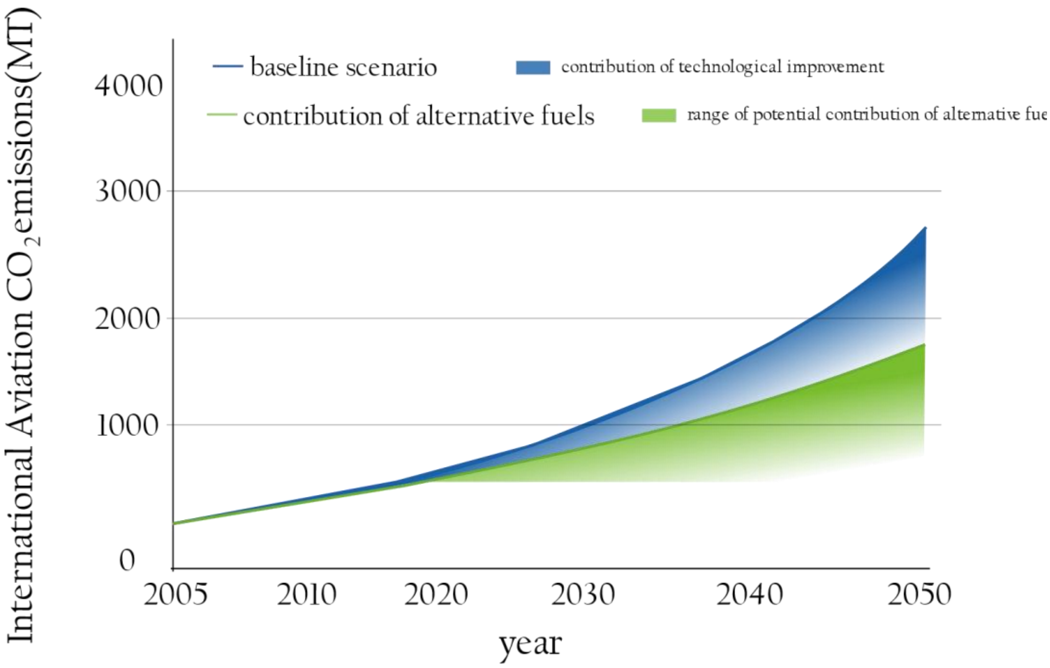

Figure 7. Aviation emissions with and without alternative fuels.

While airliners became 70% more fuel-efficient during the last half of the 20th century, overall emissions rose significantly as air travel grew in popularity. Despite a temporary decrease due to COVID, significant growth is expected to continue. In 2018, the International Air Transport Association (IATA) estimated that air transport numbers could double by 2038. Separately, in January 2021, Boeing announced that its new commercial airplanes will be ready and certified to fly on 100% sustainable fuels by 2030, reducing emissions by up to 80%. Similarly, in September 2020, Airbus revealed three zero-emission concept aircraft that use hydrogen as the fuel source and are expected to enter service by 2035 (AviationPros, 2020) (Boeing).

Another aspect to take into account for future aircraft is the oil price evolution and, above all, the difference in fuel price between main airports and regional airports. Fuel price is a key decision factor for airlines. Due to the COVID-19 pandemic, in 2020 the Crude oil price falls down significatively.

The speed of actual demand recovery, based on COVID-19 vaccination rates and the degree to which travel and employment conditions return to pre-COVID norms, remains an important uncertainty on the demand side (Figure 8) (Trading Economics , 2021).

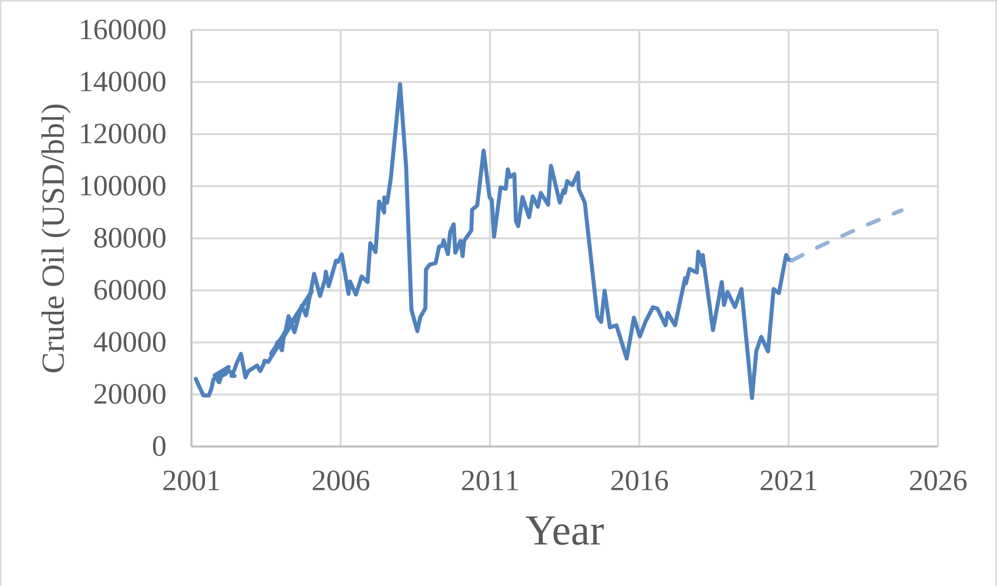

Figure 8. Crude oil price and forecast.

In light of the above it is important to consider that future alternative propulsion is important especially for regional aircraft because the fuel price is higher in regional airports than in main airports due to higher fuel transportation costs, which translates to a worldwide average extra cost of +34% (ATR, 2018).

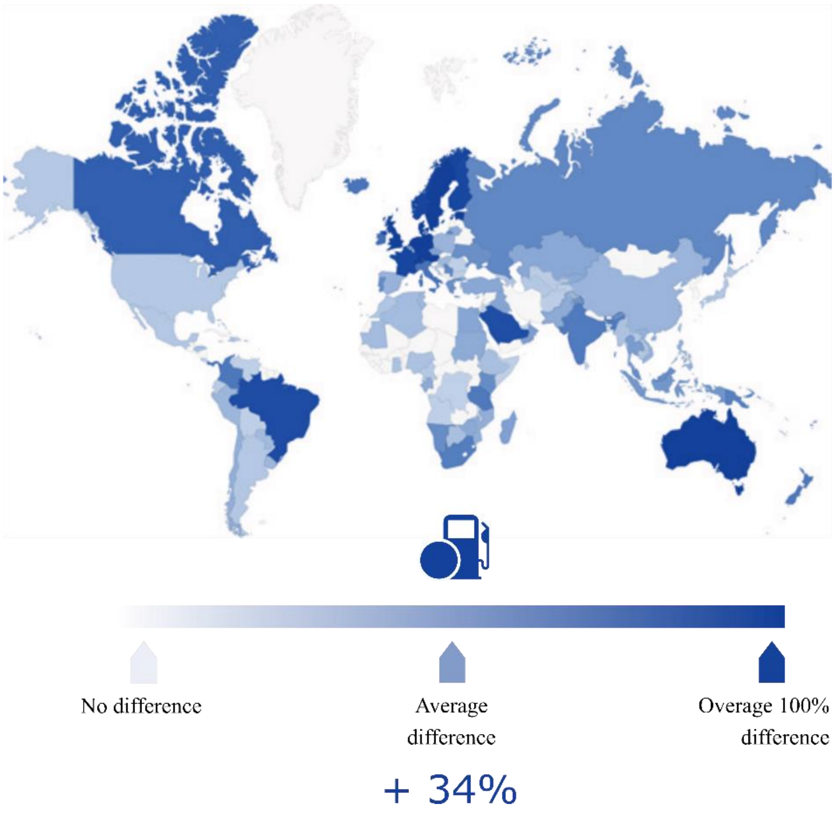

Figure 9. Difference in fuel price between main airports and regional airports.

2. Market study

2.1. Turboprop and piston engine aircraft market

Regional carriers typically operate aircraft, such as regional jets and turboprops, with a seating capacity ranging from 20 to 130 seats, on short to medium-haul routes. In the first decade of XXI century the regional aviation world fleet comprised of about 9000 units representing more than 33% of the worldwide commercial fleet and performing over 40% of total commercial flights. In a future characterized by extensive use of innovative technologies, regional aviation potential market will increase to more than 10,000 units over the 2025-2050 timeframe, doubling today market (Clean Sky 2, 2021). In the recent past the annual worldwide traffic served by regional aviation exceeded 700 billion ASK (Available Seat Kilometres). The regional aircraft market continues to be a key growth sector within commercial aviation, contributing significantly to efficiencies in the airline networks and ensuring safe and seamless mobility, while respecting environmental obligations. In the next years (Figure 10) the majority of the top 10 routes will be intra-regions. (Boeing, 2021).

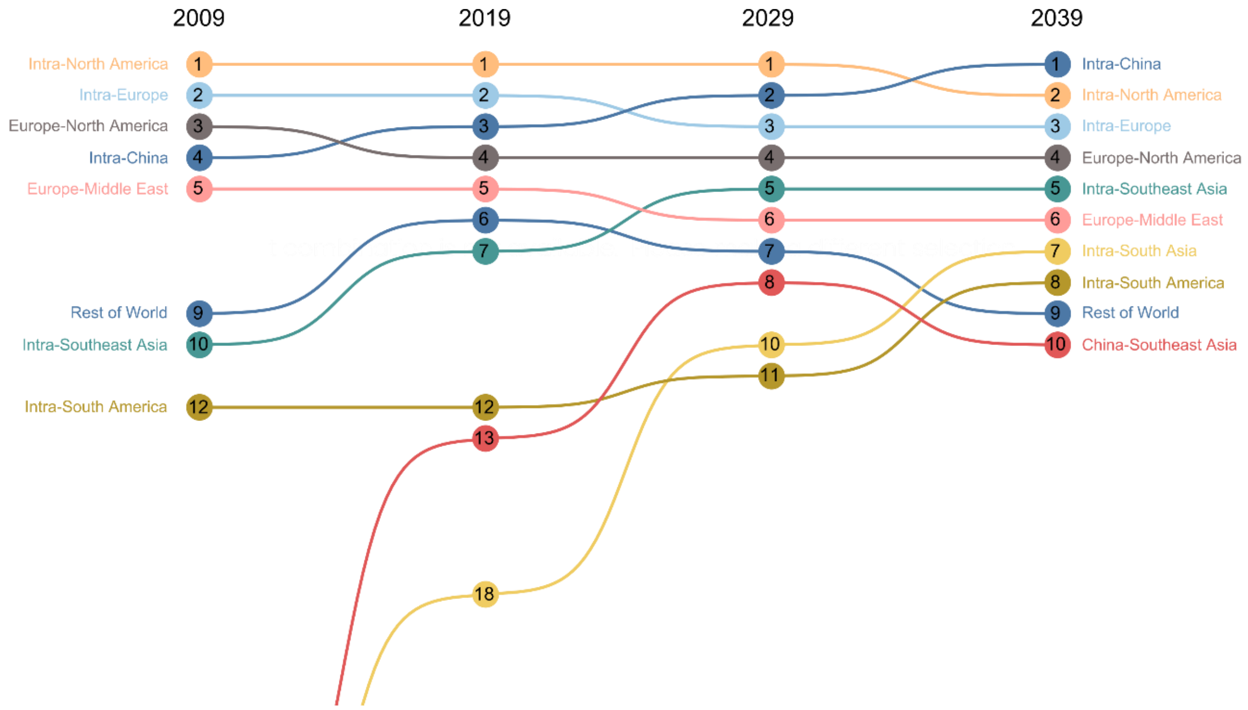

Figure 10. Passenger traffic flow forecast.

Regional aviation demonstrated its strongest traffic growth over the last two decades. In the next 20 years regional air traffic is expected to triple at an average yearly rate of 6% (compared to a 5% rate in total commercial aviation), generating, as said before, a market demand of about 9000 new regional aircraft (with a market value of about € 360 billion, averaging € 18 billion per year).

The regional market is currently led by non-European players, with the exception of turboprop manufacturer ATR (a 50/50 Joint Venture between Leonardo and Airbus Group). The integration of innovative and affordable technologies in future aircraft platforms is a key success factor for manufacturers as it increases the appeal and customer benefits, providing a better inflight experience for passengers. Furthermore, airlines derive significant economic advantages from operating modern aircraft which are more efficient, eco-friendly, easier, and cost-efficient to manage and maintain, saving money through the reduction of operating costs.

New and improved technologies positively impact all these elements, contributing to a reduction in operating costs through lower fuel burn, reduced maintenance costs, reduced navigation and airport fees because of structural weight savings due to innovative aircraft configurations and the use of lighter materials. All these benefits and economic advantages will be even more evident for regional aircraft that are typically more expensive to operate than other segments. Technological enhancements also appeal to passengers who can enjoy a better inflight experience thanks to improved comfort and lower cabin noise levels, and this means less noise in and around airports too. Clearly, investment in developing new technologies represents a fundamental differentiator for European aeronautic manufacturers in order to maintain or even to increase their competitive advantage against non-European players. Over the coming years, Europe technological leadership will gain an increasingly relevant role and will contribute to a substantial market-share increase in the regional aircraft segment with consequent job creation.

Regional turboprop market is growing fast in the last years. In fact, 58% of the current regional network has been created in the last 15 years. The bulk of growth comes from the Asia-Pacific region. Europe is once again creating routes while simultaneously growth in China is gaining momentum. (ATR, 2018). However, although some are very well populated, many countries still have poor regional connectivity, contrasting with mature European and North American markets (Figure 11).

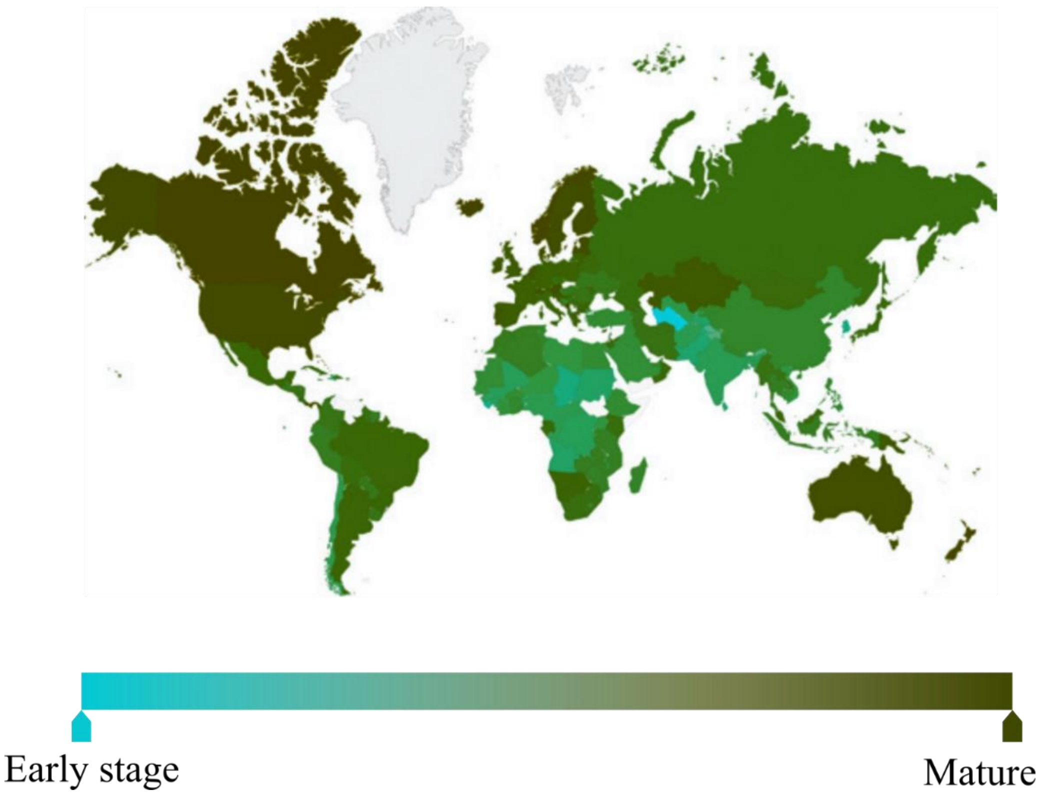

Figure 11. Regional networks maturity stage.

Many communities rely on regional aircraft to connect to other countries and regions in the world. Through an adapted technology and capacity, turboprops efficiently answer this essential market need. Almost 50% of global airport rely exclusively on regional aircraft. Regional aircraft, in fact, provide a valuable travel solution which qualitatively complements any alternative mode of ground transportation and regional air transport is a quick enabler of economic development as it requires shorter lead-time to implement connectivity (Figure 12). Either through tourism development or by establishing business, interlinking secondary and tertiary cities allows every community to be connected and benefit from world economic growth – a key component of sustainable development.

Figure 12. Different ways of transportation from Geneve (Switzerland) to Calvi (France).

2.2. Analysis of regional aircraft segment

In this section the regional aircraft segment is analyzed. An overview of aircraft from the sector is presented focusing on technical data. More in general in this section are considered designed to fly up to 100 passengers on short-haul flights, usually feeding larger carriers airline hubs from small markets. The official data sources are composed of type certification data sheets, Aircraft Flight Manuals or Pilot Operating Handbook and official statements by manufacturers and elaborated bu SMARTUP.

Table 3. Regional aircraft data.

Aircraft	Manufacturer	Year	Country	Average seats	Number of units	Powertrain
ATR 42	ATR	1984	Italy - France	42-50	436	Turboprop
ATR 72	ATR	1989	Italy - France	66-74	1500	Turboprop
CRJ100	Bombardier aerospace	1991	Canada	50	560	JET
CRJ700	Bombardier aerospace	1997	Canada	66-78	750	JET
Dash8-300	Bombardier aerospace	1989	Canada	45-56	959	Turboprop
Embraer E145	Embraer	1995	Brazil	49-55	888	JET
Fokker 50	Fokker	1985	Sweden	50-58	63	Turboprop
SAAB 2000	SAAB	1992	Sweden	50-55	63	Turboprop

Benchmark aircraft are summarized in Table 3. The first and most important step of a technical benchmark study is to define the parameters that are indicative for the product performance. Therefore, it must be understood how the product works and how customer benefit is generated. First of all the maximum number of seats are compared in order to localize the GENESIS project in the reference market. Then the most interesting parameters are analyzed. The take-off performance is compared to the Maximum Take Off Weight (MTOW). Take off distances of regional airliners is often disregarded, because they are often operated from large airports with runways designed for bigger aircraft. However, economic feasibility studies show that point to point connections which are not covered by narrowbody airplanes can be more profitable and a competitive niche for regional aircrafts. The shorter the required runway the more airports can be part of the route network. A truly relevant parameter is the range because it influences the routes.

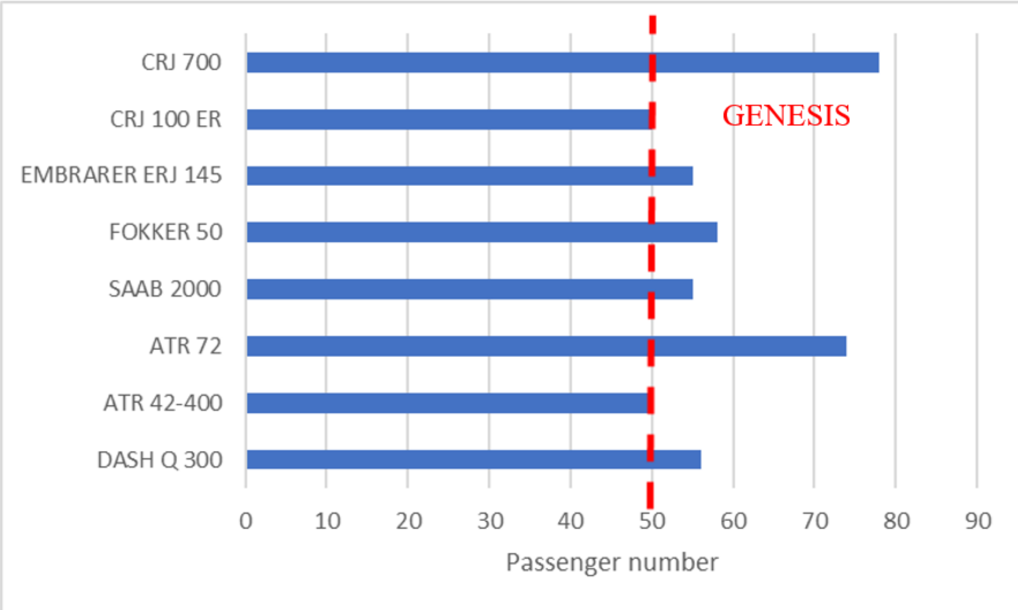

Figure 13. Aircraft regional segment data comparison – Maximum number of seats.

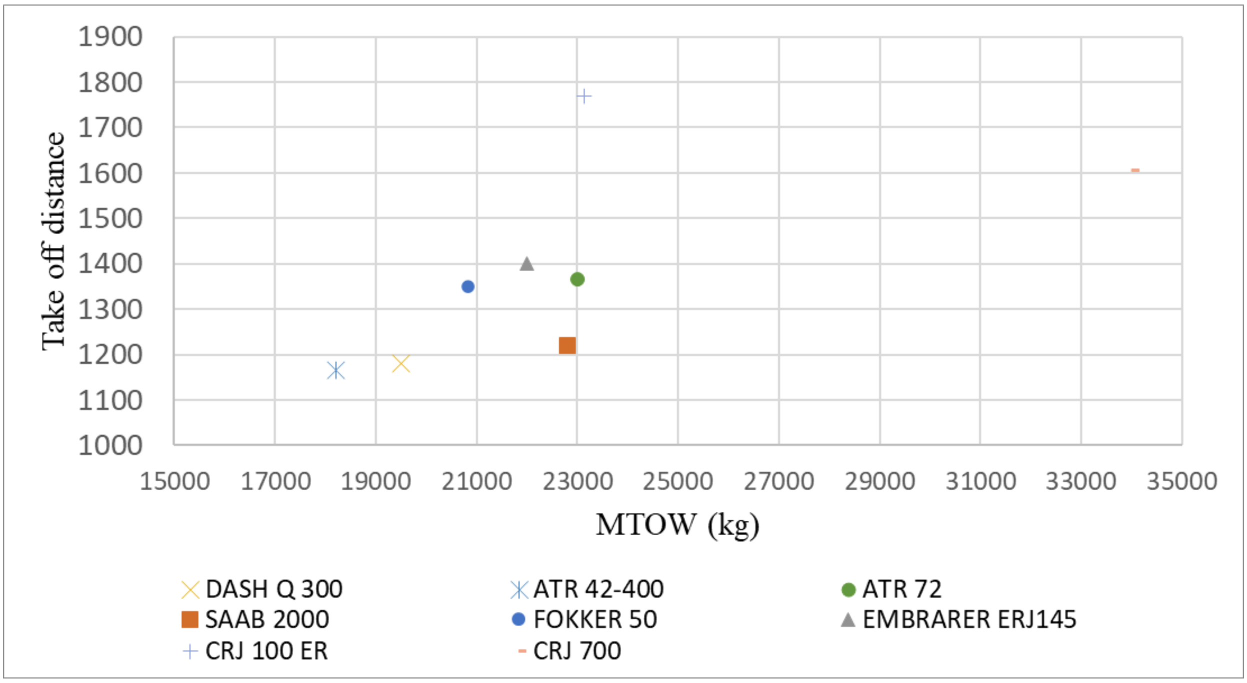

Figure 14. Aircraft regional segment data comparison – take off distances.

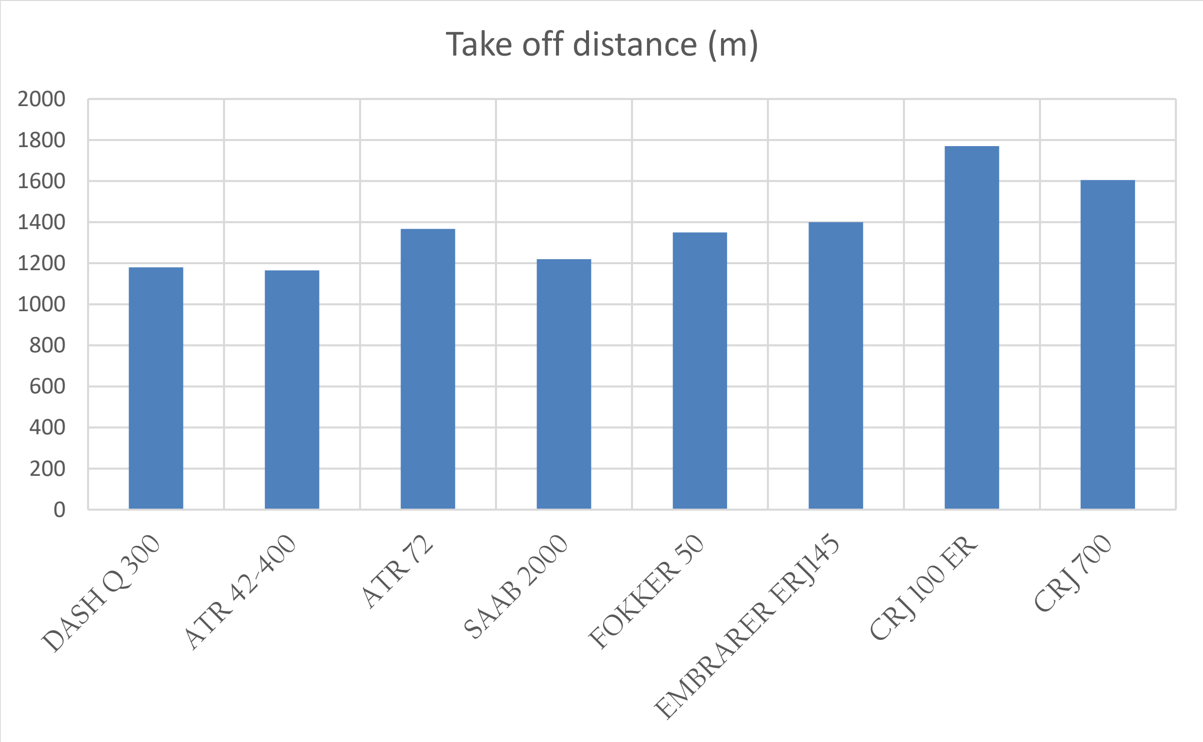

Figure 15. Aircraft regional segment data comparison – take off distances.

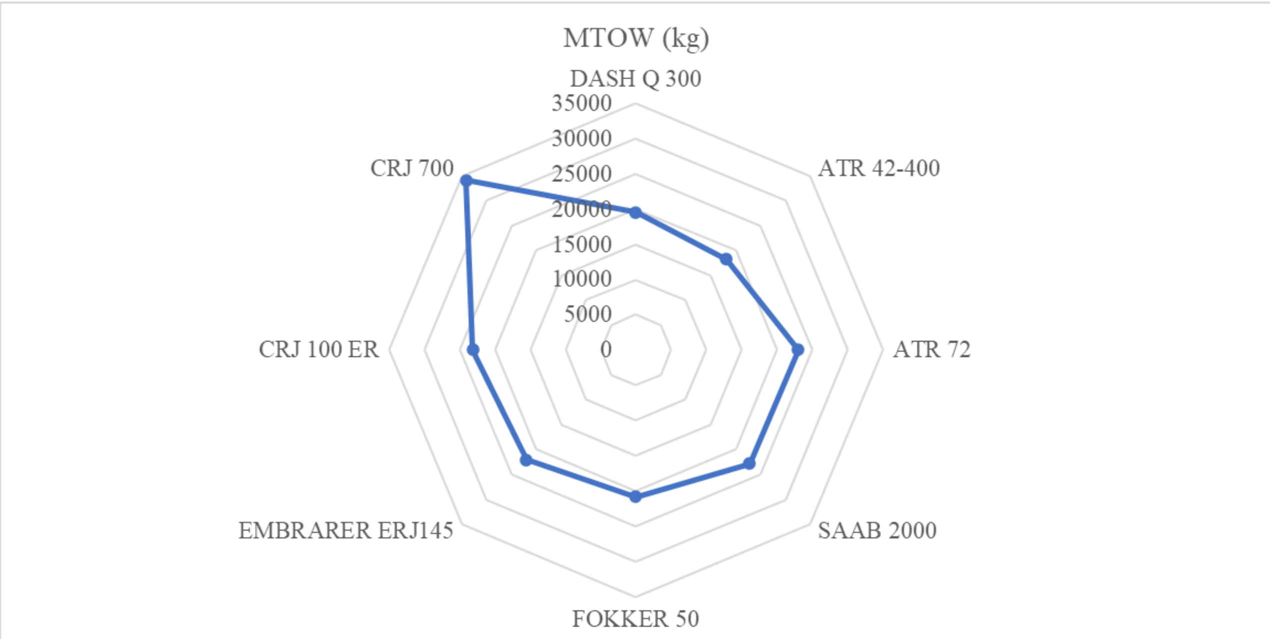

Figure 16. Aircraft regional segment data comparison – maximum take-off weight.

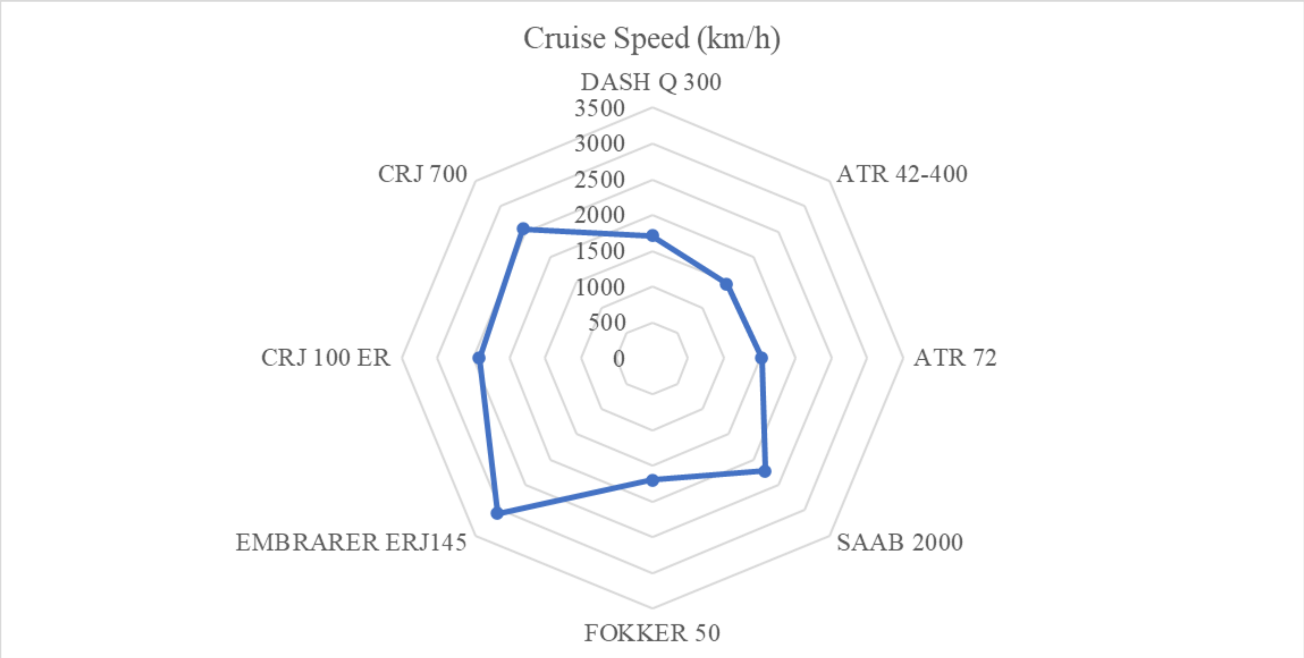

Figure 17. Aircraft regional segment data comparison – Cruise speed.

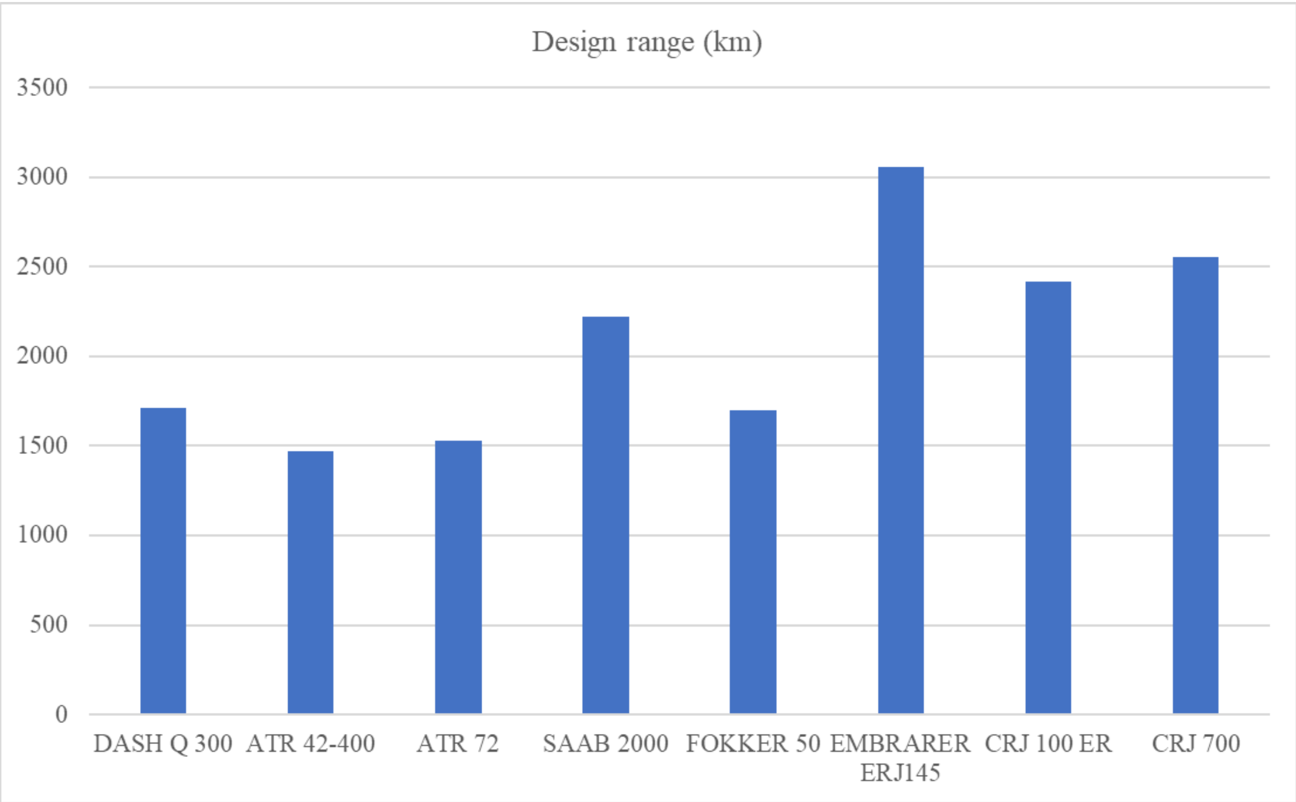

Figure 18. Aircraft regional segment data comparison – Design range.

Another important aspect is the Take off field length. Concerning that, the World airport runway have been considered (Figure 19. World airports runway . In order to serve more than 90% of world airport, the TOFL should be lower than 1200m (Figure 19). In fact, as shown in Figure 20, less than 10% of world airports have a runway shorter than 1200m.

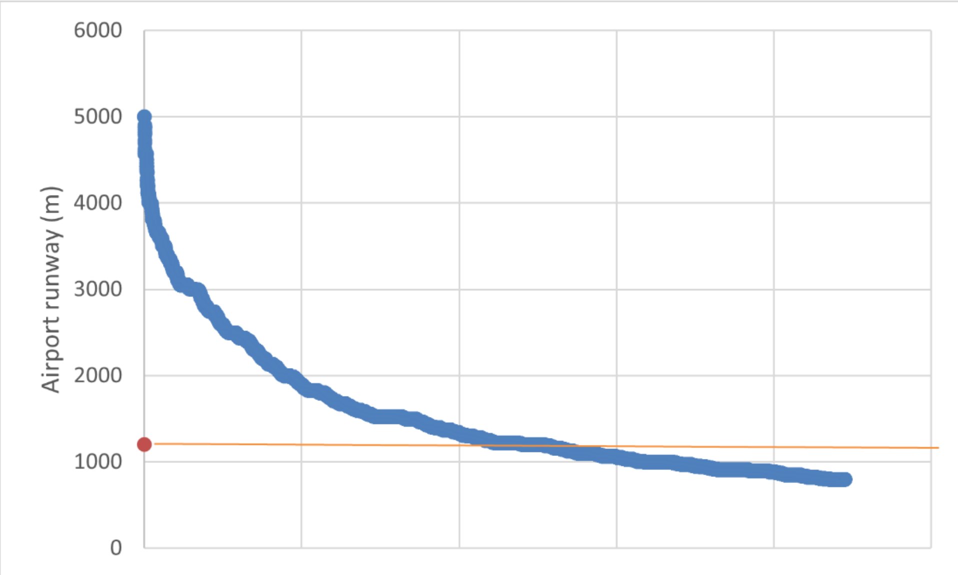

Figure 19. World airports runway **(https://ourairports.com/, 2021)**.

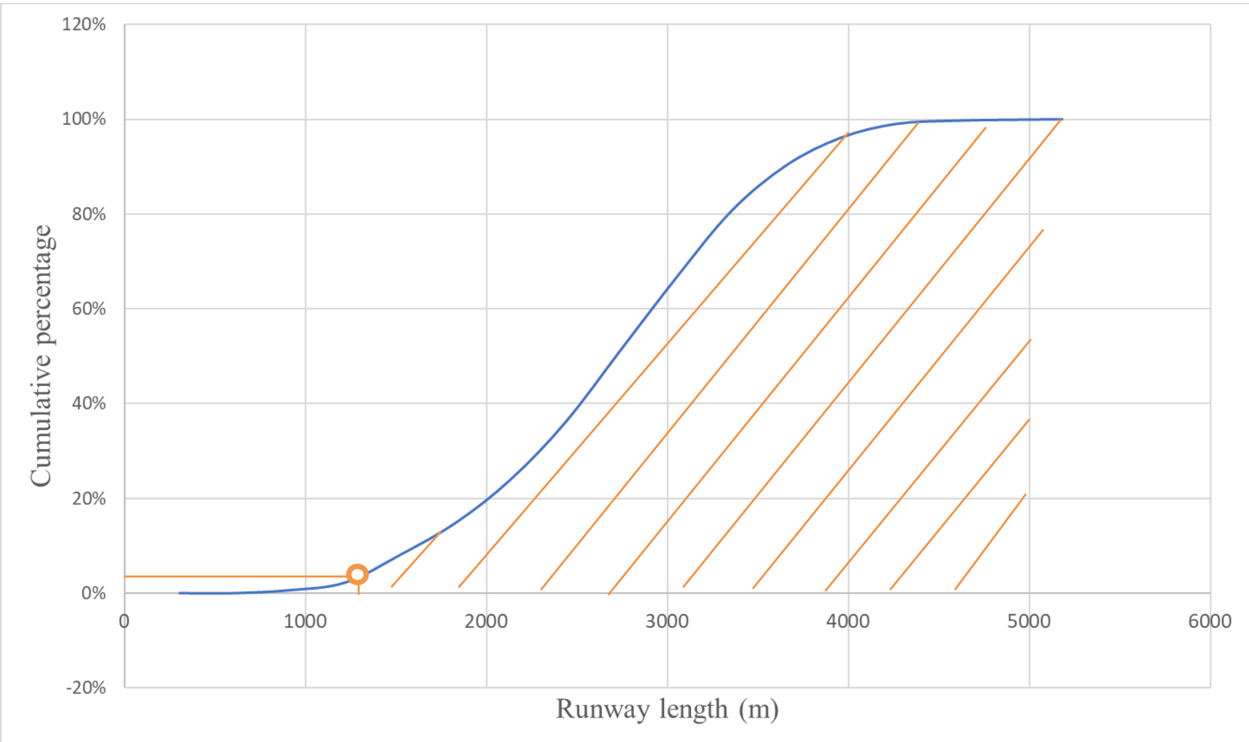

Figure 20. World airports runway, cumulative percentage.

2.3. COVID-19 influence on the segment

The sudden halt imposed on the aviation industry by the Covid-19 crisis hit the sector hard. In April 2020, two-thirds of the global commercial aviation fleet sat idle on the tarmac, while passenger traffic was down 90% year-on-year. Pre-Covid-19 business travel traffic amounted to $1.5trn a year or around 1.7% of global GDP and IATA Economics' Chart of the Week Five years to return to the pre-pandemic level of passenger demand, 2019 levels recovered by 2024 Today, the aviation industry is slowly rebounding, led by domestic travel. The short-term scenario is based on a slower than expected recovery in economic activity from the virus. As a starting point, the pandemic is assumed to be worse (i.e. of longer duration) than that anticipated in the base case. The Asia Pacific and Africa&Middle East regions are expected to recover more quickly than the more mature air transport markets of North America and Europe.

The pandemic has also an indirect impact on aviation. Earlier this year, dozens of pilots reported making mistakes, such as taking multiple attempts to land, to NASA's Aviation Safety Reporting System, with many citing rustiness as a factor on returning to the skies Unruly behavior of airplane passengers is increasingly a concern, particularly in the United States. In a typical year there are around 150 reports of passenger disruption on aircraft. By June 2021 there had been 3,000 according to the Federal Aviation Administration – the majority involving passengers refusing to wear a mask. The report notes that unruly passengers may later claim they were discriminated against by the airline in these cases even when in the wrong – a trend insurers need to stay on top of. Although a large proportion of the world's airline fleet have been – and are still – parked during Covid-19, loss exposures do not disappear.

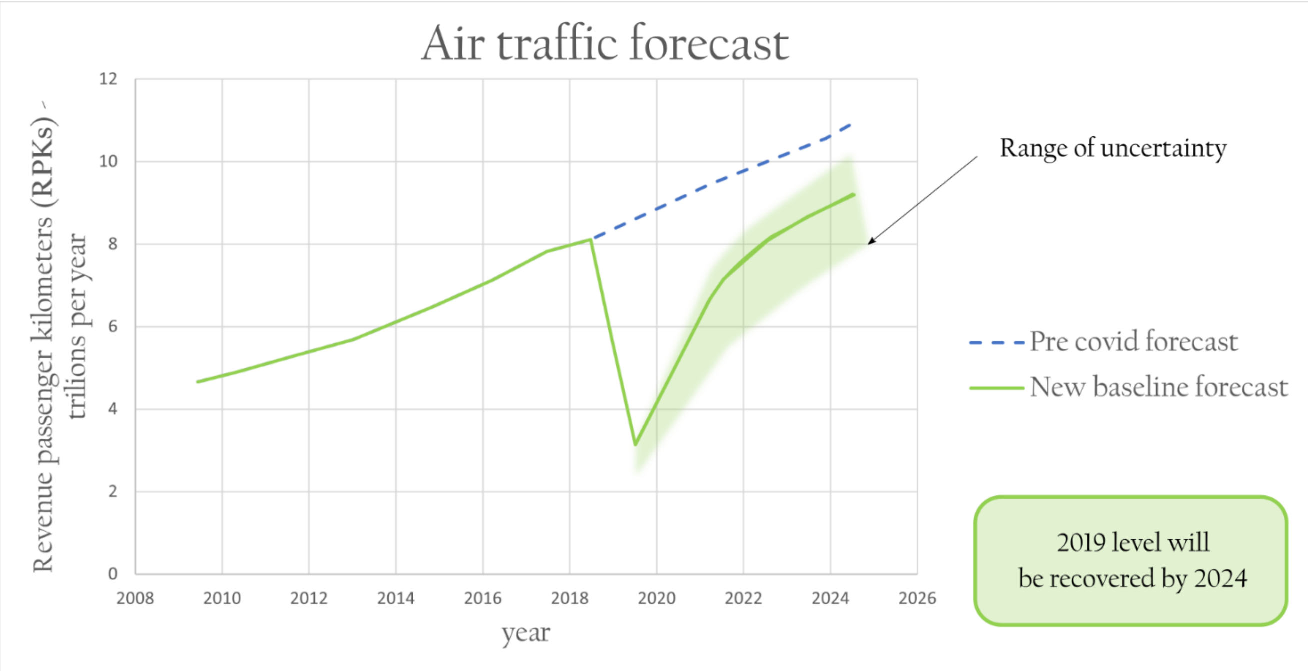

Figure 21. Air traffic forecast and COVID-19 impact.

3. Genesis TLARs

GENESIS TLARs have been defined by SMARTUP and UNINA, starting from the reference mission for the aircraft and the reference values from benchmark aircraft taking into account economic an infrastructure-related data. The chapter will close with an initial set of TLARs defined for GENESIS Scientific and technical recommendations for TLARs

3.1. Scientific recommendations for TLARs

The most important link between the market scenario analysis and the TLARs is the definition of the reference mission. It defines the average operation of an aircraft and can be used to execute performance calculations. The future analysis scenario is the result of a deep analysis into the international transport network and data form air segment market and passenger demand.

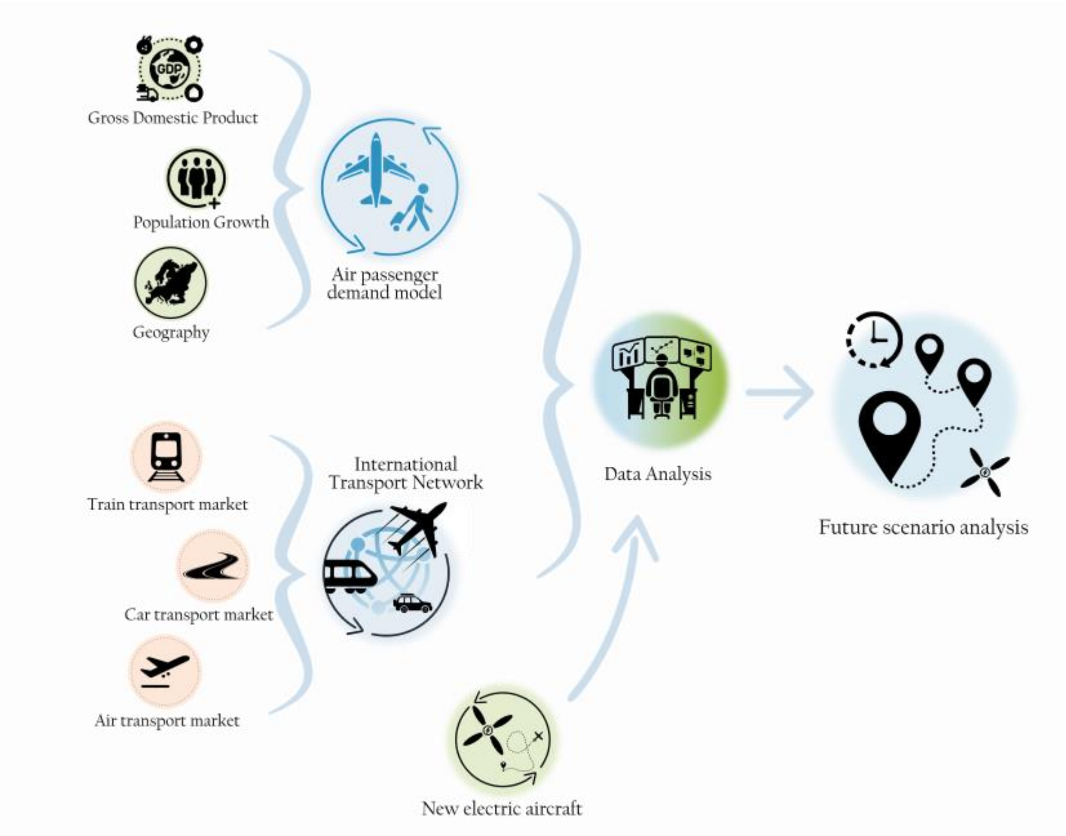

Figure 22. Future scenario analysis and derivation of TLARs process.

Over many regional transport systems, high speed rail is competing with air transportation, often considering time and distance factors. Airports are usually located far from city centers, while conventional and high-speed train stations are much closer. For short distances of less than 150 km, conventional rail services are usually more competitive (air transport is almost never flown over these distances) than high speed. This is mainly due to higher frequencies of services for conventional rail.

The main service window for high-speed rail is between 150 and 775 km, a segment over which it generally has a time advantage over air transportation. For distances over 800 km, air transportation is usually more advantageous. However, if there were no high-speed rail services, air transportation would be more advantageous over distances of 350 km (Figure 23) (Gleave, 2004). These considerations define the design mission of 600Nmi of GENESIS project. Take off field length has been chosen lower than the mean of benchmark aircraft (1362m) in order to serve more regional airports.

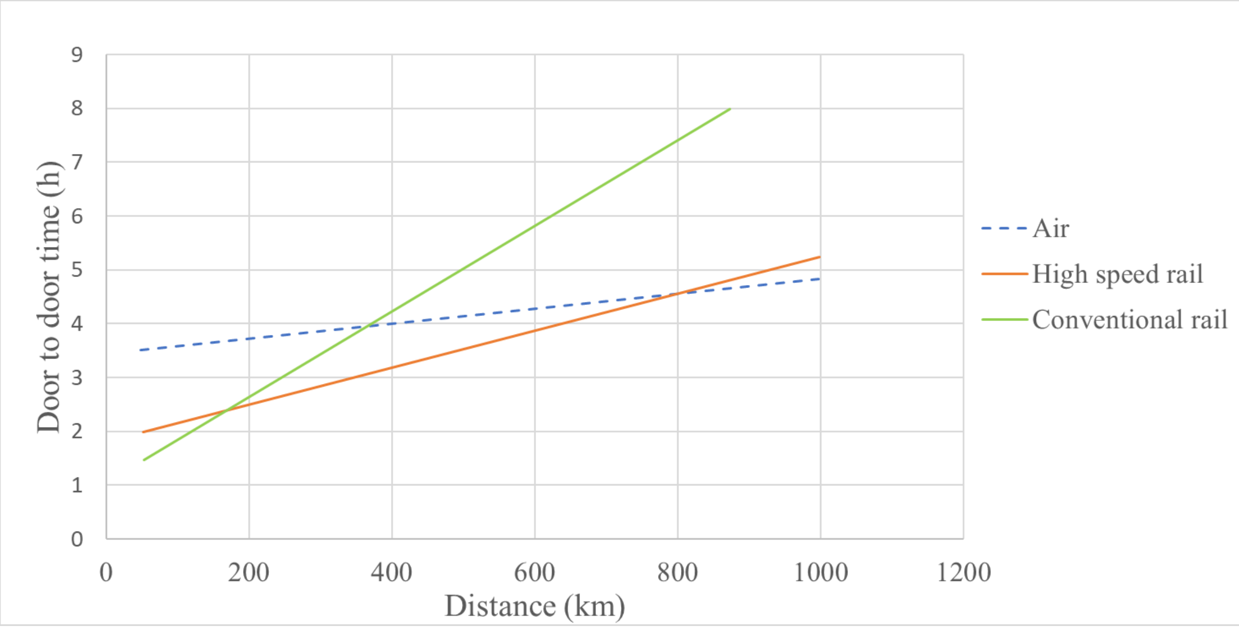

Figure 23. Breakeven Distance between conventional rail, high speed rail and air transportation.

3.2. TLARs suggested for GENESIS

In the light of the above-mentioned considerations, GENESIS TLARs has been defined. Table 5 provides an overview of suggested TLARs for GENESIS. This set of requirements has to be regarded as an initial design approach that forms a starting point and needs to be challenged, shaped, and detailed during the course of design. As regards the three time perspectives: short term (2020-2035), medium term (2035-2045) and long term (2045-2050+), TLARs are assumed constant, while different technologies will be identified in the next paragraph relying on UNINA experience. In particular, Distributed electric propulsion (DEP) has been identified as the most promising innovative technology, more suited to the short-term time horizon, while fuel cells will be mature for further time horizons. The system weight reduction led to the possibility to increment the passenger number with a moderate increment of MTOW. This is the reason why in the medium and long-term it is possible to modify the MOTW requirement to < 27000kg in order to increment the passenger number (de Vries, Brown, & Vos, A Preliminary Sizing Method for Hybrid-Electric Aircraft, 2018).

As far as emission objectives the target is the prescribed from Clean Sky 2 (Clean Sky 2, 2021) and reported in Table 4.

Table 4. Emission objective for regional transport in GENESIS project.

Time horizon	CO_2 reduction	NO_X reduction
Short-term	-27%	-46%
Medium-term	-54%	-98%
Long-term	-100%	-100%

Table 5. Initial set of GENESIS TLARs.

Description	Value	Unit	Notes	Notes for medium and long term time horizon
Design mission	600	Nmi		
Typical range	200	Nmi		
Time to Climb (Design Mission)	13	min	1500 m - 200FL @ MTOW	
Cruise Speed	295-300	KTAS	@200 FL	
Take-Off Field Length	<1200	m	At SL, ISA and MTOW	
Landing Field Length	<1200	m	At SL, ISA and MLW	
Max Payload	4750	kg	50 pax – 95 kg per pax	
Design Payload	4560	kg		
MTOW	<24000	kg		<27000 kg

4. Introduction to Hybrid-Electric Aircraft Design

4.1. Electric Propulsion Systems

The growing sensitivity towards environmental sustainability drives the demand for a revolution in the aerospace propulsion sector, requiring a reduction in carbon emissions that cannot avoid the involvement of disruptive technologies and the use of alternative energy sources. The major emissions of modern aircraft engines are carbon dioxide, nitrogen oxides, sulfur oxides, unburned hydrocarbon, carbon monoxide, particulate matter, and soot. The design of new concepts that employ hybrid-electric propulsion architectures, in this sense, represents the most promising solution to the problem. Hybrid-electric propulsion systems are an effective way to reduce pollutant emissions as long as the energy sources are renewable. Electric propulsion can be all-electric, hybrid-electric, and turbo-electric. There are several variants of the logic schemes of an electric propulsion system (Felder, 2015; Orefice, Della Vecchia, Ciliberti, & Nicolosi, 2019; de Vries, Brown, & Vos, A Preliminary Sizing Method for Hybrid-Electric Aircraft Including Aero-Propulsive Interaction Effects., 2018; Ciliberti, Orefice, Della Vecchia, Nicolosi, & Corcione, 2019). A simplistic representation of the hybrid series/parallel electric powertrain is given in Figure 24.

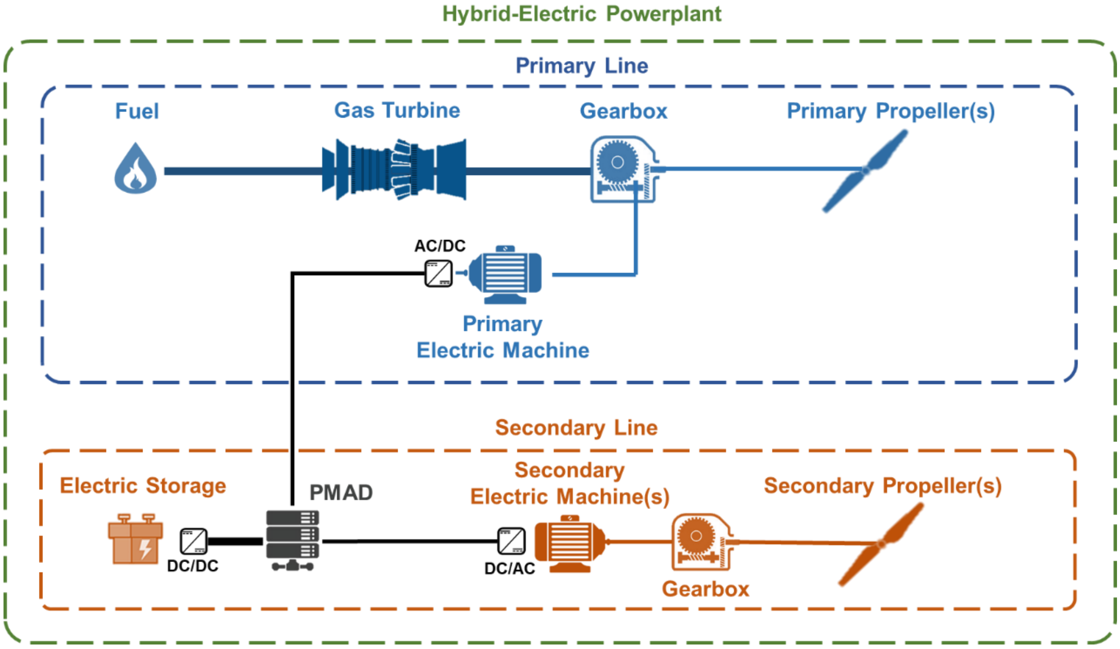

Figure 24. Hybrid-electric propulsive scheme.

The presented diagram relates to the case of two energy sources, where the thermal power source is marked as *primary*, and the electric energy storage as a *secondary* source. The primary line is generally composed by a *thermal engine* capable of producing mechanical power from the combustion of carbon fuel. This power is transmitted to a shaft which drives thrust-producing *propellers*, and a *gearbox* can be used to match the operating rotational speeds. However, part of the mechanical power is redirected towards an *electric machine* where it is converted into electric power. An AC/DC converter turns the alternate current into direct current, which reaches the secondary line. Here, the *electric storage* system releases additional electric energy, which is recombined by a *power management a distribution system* (PMAD). Finally, the direct current reaches the secondary electric machines where it is converted into mechanical shaft power. To give an idea of the generality of the scheme presented above, the connection between the two propulsive lines can also be read in reverse. Part of the battery energy can be sent to the primary electric machine and converted into mechanical power which helps move the primary thrusters. The general scheme of Figure 24 is used in literature to deduce all the main concepts of propulsive architecture, which will be briefly explored in the next section. In order to quantify the hybridization level of the system, two different parameters can be used. The *supplied power ratio*, Φ, is defined as the ratio between the electric energy power and total power supplied:

$$\Phi = \frac{P_{\text{E-storage}}}{P_{\text{fuel}} + P_{\text{E-storage}}} \quad \textbf{(1)}$$

The second parameter represents the ratio between secondary powertrain propulsive power and total propulsive power and is named the *shaft power ratio*, φ. It is very useful when dealing with high-lift propellers and distributed electric propulsion, since it quantifies the use of such systems:

$$\varphi = \frac{P_{Shaft,2}}{P_{Shaft,1} + P_{Shaft,2}} \quad \textbf{(2)}$$

In the previous formula, the subscript 1 indicates the group of primary thrusters, while the subscript 2 relates to the secondary propellers. Note that the definition chosen concerns the shaft powers and not the propulsive powers, so the real distribution of propulsive power could be slightly different due to the different efficiency of the propellers. A third hybridization parameter is also defined as the ratio between the distributed propulsive power (or thrust) and the total propulsive power (or thrust):

$$\chi = \frac{1}{1 + \frac{\eta_{Prop,1}}{\eta_{Prop,2}}\left(\frac{1-\varphi}{\varphi}\right)} \quad \textbf{(3)}$$

The main difference between Eq. (2) and Eq. (3) lays is in the propulsive efficiencies, $\eta_{Prop,1}$ and $\eta_{Prop,2}$, which are generally affected by the external flow conditions. In this sense, key parameters are the air speed, the altitude and the temperature. Also, the throttle setting and the rotational speed influence these parameters. However, propellers are not the only elements to be characterized by an efficiency.

Hybrid and electric vehicles are provided with high voltage battery packs that consist of individual modules and cells organized in series and parallel. A *cell* is the smallest, packaged form a battery can take. A *module* consists of several cells generally connected in either series or parallel. A *battery pack* is then assembled by connecting modules together, again either in series or parallel. Electrochemical cells store chemical compounds holding a voltage difference between the electrodes. The battery provides electric energy with a chemical reaction when the electric circuit at its poles is closed. Cells convert the energy stored in the chemical bonds directly into electricity, without producing heat or thermal energy as an intermediate stage of the energy conversion process. Because of this, electrochemical cells are not subjected to the Carnot limitations, hence their efficiency in releasing energy can be very high. Current batteries can store below 250 Wh/Kg. For regional hybrid-electric turboprop specific energies higher than 500 Wh/kg would be needed. For an all-electric system, the required specific energy may be around 2,000 Wh/kg, if the actual design range are to be kept (de Vries, Brown, & Vos, A Preliminary Sizing Method for Hybrid-Electric Aircraft Including Aero-Propulsive Interaction Effects., 2018; Strack, Pinho Chiozzotto, Iwanizki, Plohr, & Kuhn, 2017; Michaelides, 2012; The National Academies of Sciences, Engineering and Medicine, 2016). While theoretical specific energy is much higher than this, in practice the attained value will be significantly lower, because of the added weight of current collectors, electrolytes, separators, battery cases, and terminals. Furthermore, the requirement to simultaneously achieve long cycle life, low cost, and acceptable safety greatly increases the complexity of the overall challenge. Lithium-ion batteries currently dominate the market in both consumer electronics and electric vehicles (Table 6). A trend on specific energy derived from NASA/Boeing Sugar study indicates that an increment of 7.6% per year is needed in order to achieve 750 Wh/kg by year 2030 (German, Bradley, McDonald, & Vos, 2018). Although additional improvements are foresighted, even 500 Wh/Kg within year 2035 seems optimistic.

Table 6. Trends in future batteries at cell level by year 2035 **(Zamboni, 2018)**.

	Li-Ion	**Li-S**	**Li-O2,open**	**Li-O2,closed**
Specific Energy [Wh/kg]	250-350	600-700	800-1500	600-1200
Specific Power [W/kg]	500-600	350-500	300-400	300-400
Energy Density [Wh/l]	600-800	300-350	1000-1700	1000-1600
Charge/Discharge efficiency [%]	90-95	70-90	60-85	60-85
Cycle life # [cycles]	1000-3000	1000-2500	500-1000	500-1000
Degree of Discharge [%]	70-90	90-100	70-90	70-90

Lifetime [years]	7-15	7-14	5-10	5-10
Cost ($ 2010) [$/kWh]	250-350	250-500	400-800	300-700
Uncertainty [-]	low	medium	high	high

To aspire to a competitive design that also looks at the needs of the market, the values proposed in Table 6 will be taken as the technological basis for the short-term time horizon. The assumptions for the medium-term and for the long-term are reported in Table 7, in terms of energy density and power density. These assumptions must be confirmed or changed by the results produced in the context of WP2.1. The operating life and cost of the battery are to be understood as driving factors, to be optimized to reduce the economic and environmental impact of the aircraft.

Table 7. Preliminary assumptions on technological level of Li-Ion batteries for all time horizons.

	2025-2035	2035-2050	2050+
Specific Energy [Wh/kg]	250	350	500
Specific Power [W/kg]	500	1000	1000
Energy Density [Wh/l]	600	800	800

For conceptual design purposes, a more simplified approach than those described in the literature will be used, while ensuring that most phenomena are captured, and the error is minimized. For the correct battery modelling, specific curves representing the discharge characteristics of the individual cells will be interrogated. The knowledge of these curves replaces the pre-existing knowledge of the internal characteristic parameters required from the manufacturer by the above-mentioned models (e.g., the impedance values). An example of battery discharge curves is given in Figure 25, where each curve relates to a different C_{Rate} value (i.e., current intensity). The voltage response of the cell can thus be interpolated or extrapolated linearly starting from the assigned curves, given a value of the state of charge and the C_{Rate}. A $C_{Rate} = 1$ means that the discharge current will discharge the entire battery in 1 hour, and the total discharge capacity is equal to the C_{Rate} times the current intensity. Transient responses are not considered; however, they are believed to be reasonably negligible.

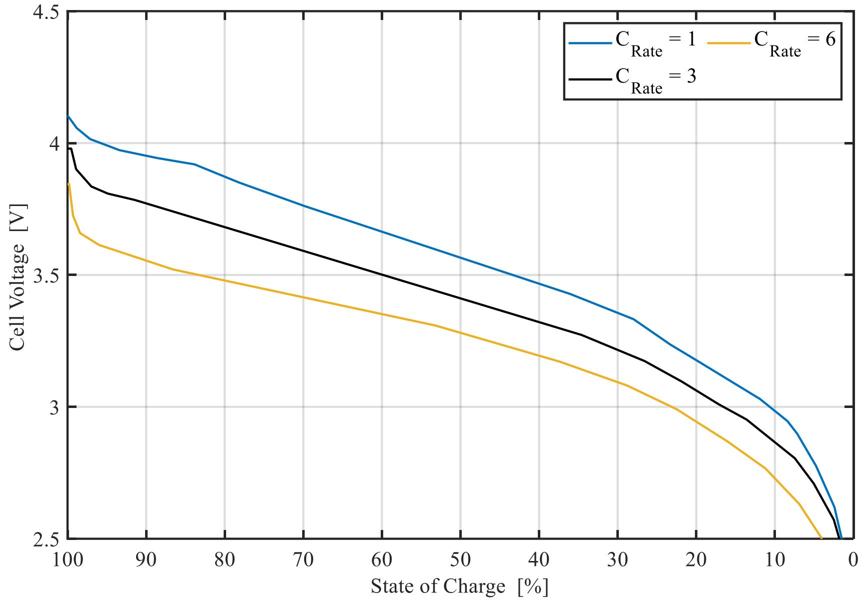

Figure 25. Example of battery capacity versus battery voltage at different discharge rates.

A very similar reasoning applies to fuel cells, for which UNINA needs operating curves of the single stack in order to model their operation (an example is shown in Figure 26).

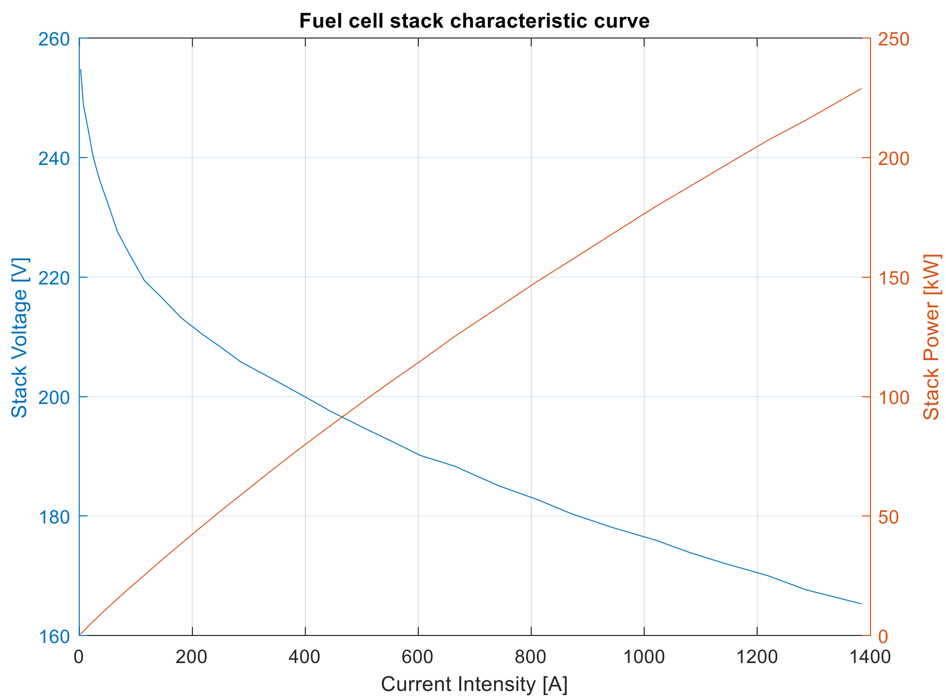

Figure 26. Characteristic curves of a SINAVY FCM120 PEM fuel cell stack[1].

4.2. Powerplant Architecture

[1]https://assets.new.siemens.com/siemens/assets/public.1535009488.28615cde70250d0e81b68ba466bd77d7f5c68c73.sinavy-pem-fuel-cells.pdf

The scheme of Figure 24 is useful to generally describe a hybrid-electric powertrain architecture with up to two different energy sources. Keeping the hypothesis of primary propulsive line supplied by a thermal engine, 9 different hybrid concepts can be deduced by particularizing the scheme above. These concepts can be visualized in Figure 27.

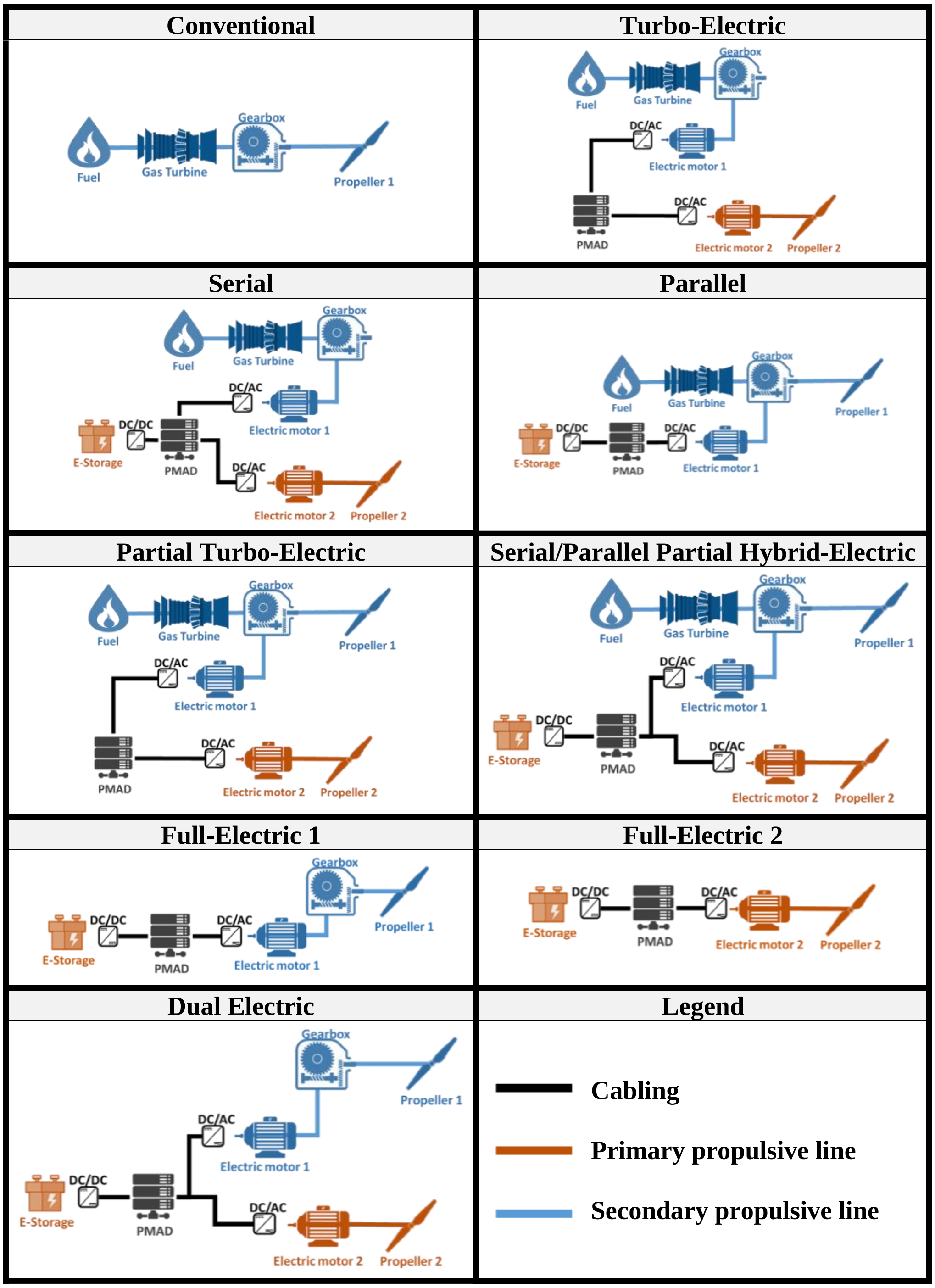

Figure 27. Different hybrid-electric architectures

In synthesis, electric propulsion can be **all-electric**, **hybrid-electric**, and **turbo-electric**, thus the 9 different concepts can be classified as follows:

- **Conventional**
- **Full-electric**
- **Turbo-electric**
  - Full turbo-electric
  - Partial turbo-electric
- **Hybrid-electric**
  - Parallel hybrid
  - Series hybrid
  - Series/parallel partial hybrid

Full-electric concepts employ high-efficiency, light-weight motors to drive propellers. The latter can be coupled directly to the electric motors, or by means of a gearbox if the rotation speed are not compatible. All power is supplied by electric storage systems, or open electrochemical systems generating electric power (e.g., fuel cell systems). *Turbo-electric* systems use only thermal energy coming from fuel combustion and convert it into electric energy by means of separately-located generators, which is then converted again into mechanical power by means of electric motors. On the one hand, turbo-electric systems are affected by low global efficiencies due to the multiple energy transformations. On the other hand, this concept can result in much more flexibility when it comes to optimizing the arrangement of the system components on board, and to reducing weight. For example, one can imagine a propulsive configuration with a single turbine carried in the fuselage, which powers a number of electrically-driven propellers. Finally, *hybrid-electric* concepts are characterized by both energy sources, thus they offer the greatest opportunities for an optimization both at system and aircraft level. The propulsion power in a *parallel hybrid-electric* system is achieved by directing both thermal and electric power towards the same thrust generators, via the power management and distribution system. The higher the degree of hybridization, the most this power comes from the electric-storage. Increasing degree of hybridization allows to downsize the thermal engine, and potentially to save weight besides to reduce carbon emissions. Furthermore, electrical systems tend to be characterized by higher levels of efficiency leading to less energy waste. On the other hand, the technological level of batteries hardly allows to entirely replace thermal engines due to their limited gravimetric power and energy density. The same reflections apply to *serial* hybrid-electric systems, where the mechanical power generated by the thermal engine is all converted into electrical energy, as in the case of turbo-electric concepts. In this case, this power is added to that provided by the electric storage. The serial hybrid-electric, while presenting lower efficiency than the parallel hybrid-electric concept, combines the advantages of a turbo-electric architecture with non-zero hybridization levels. Finally, the *serial/parallel partial* hybrid-electric concept does not simplify anything compared to the general scheme seen in Figure 24, preserving all the elements and their interconnections. The generality of this concept allows for a greater optimization of the mission strategy, even allowing to reverse the operating mode of the elements. For example, the primary electric machine can reverse the direction of the energy flow as needed, working as a motor or generator depending on the flight phase. Furthermore, in the phases in which a lot of propulsive power is not required (e.g., descent) some or all of the thrusters may no longer be required as thrust-generators, but rather as absorbers of energy from the external flow. Energy from windmilling propellers and/or from fuel combustion, when exceeding the power needs, can also be used to recharge the battery. Depending on the efficiencies of each element, which depend on external and operational conditions, it is possible that not all energy flow directions represent physical solutions. A trivial example is when for a given propulsive power demand, both power sources could be forced to supply power and the battery cannot be recharged. To better manage all possible combinations, and to provide a wider overview of the propulsive architectures, it is convenient to define 9 different *operating modes* corresponding to 9 different combinations of the direction of the incoming and outgoing powers in the different elements. The operating modes are described in Table 8, based on different behaviors of propellers, electric storage and primary electric machine. Each operating mode can be treated separately, by means of proper systems of linear equations generally referred to as *powertrain equations*, which also consider the efficiencies of the individual components of the powertrain as operating conditions vary.

Table 8. Hybrid-electric powertrain's operating modes.

Operating Mode	Primary Propeller(s)	Secondary Propeller(s)	Electric Storage	Primary Electric Machine(s)
1	Thrust	Thrust	Discharge	Generator
2	Thrust	Thrust	Charge	Generator
3	Thrust	Harvest	Charge	Generator
4	Thrust	Thrust	Discharge	Motor
5	Thrust	Harvest	Charge	Motor
6	Thrust	Harvest	Charge	Motor
7	Harvest	Thrust	Discharge	Generator
8	Harvest	Thrust	Charge	Generator
9	Harvest	Harvest	Charge	Generator

Finally, a brief mention should also be made of the propulsion scheme that will be adopted as a reference for the hydrogen-based configurations. In the case of use of three propulsive sources, namely kerosene, batteries and hydrogen, the SOFC or PEM fuel cells should be imagined arranged in parallel with the electric-storage devices as they both supply electricity in the form of direct current. Hydrogen consumption will be evaluated at each time step according to the power required by the fuel cells and the operating conditions. In this sense, the fuel cell system model is expected as a result of WP2. In case of deep use of fuel cells, i.e., complete replacement of the thermal system with hydrogen fuel cells, the architecture will be changed with respect to the models proposed in literature, as shown in Figure 28. The operating modes are reduced to the subset presented in Table 9.

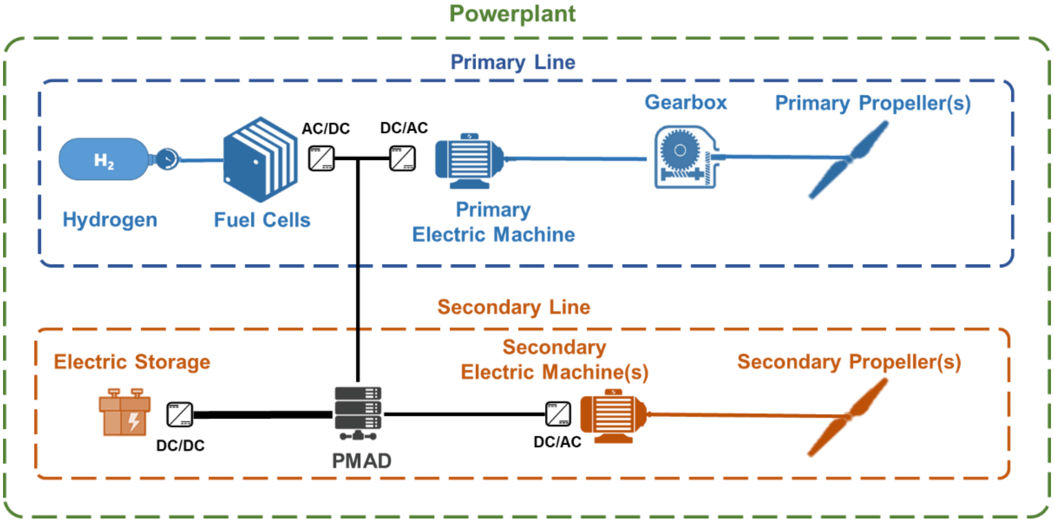

Figure 28. Fuel cell based powerplant architectures.

Table 9. Fuel cell based powertrain's operating modes.

Operating Mode	Primary Propeller(s)	Secondary Propeller(s)	Electric Storage
1	Thrust	Thrust	Discharge
2	Thrust	Thrust	Charge
3	Thrust	Harvest	Discharge
4	Thrust	Harvest	Charge
5	Harvest	Thrust	Discharge
6	Harvest	Thrust	Charge
7	Harvest	Harvest	Charge

4.3. Aero-propulsive interactions

Improvements in aerodynamics have direct impact on aircraft performance. Research in the aerodynamic field has always been pushing aeronautical technology to ever higher levels. Improvements in terms of aerodynamic can be achieved by adopting innovative technologies, guaranteeing a positive impact on main performance, and strongly contributing to reduce product cost and improve operability. When dealing with disruptive technologies, the most problematic obstacle for the designer is represented by the lack of established design methodologies that allow the real advantages of new concepts to be reliably ascertained. For the purposes of the GENESIS project, it is essential to know how to model and capture the effects of aero-propulsive interaction, which have the potential to reconcile lower emissions with real benefits in terms of performance, when compared to conventional aircraft of the same market segment. Different powertrain concepts can be identified to improve the overall efficiency:

1. Increasing the dynamic pressure over the wing above free stream during approach to allow for increased design wing loading.
2. Installing propellers at the wing tips to reduce induced drag.
3. Placing propulsors in the wake of aircraft components.

The first mechanism is based on the idea of distributing the propellers spanwise and upstream of the wing. In this case, we generally speak of *distributed electric propellers* (DEP). Another method by which distributed propeller wing systems can increase the efficiency of small aircraft concepts is to place the propellers on the *wing tips*. One may object that if these techniques can enable large performance benefits, then current aircraft would employ such strategies. The reasons for not using such systems largely stem from the characteristics of conventional motors, i.e., it is simply impractical to deploy many conventional motors due to their size and weight. However, by using distributed electric motors, many of these practical design considerations may no longer be barriers to implementing wingtip mounted propellers or any other technique.

4.4. Distributed Electric Propulsion

As the wing sections in the propeller wakes experience an increase in flow dynamic pressure, the generated lift locally increases compared to normal freestream, which makes the wing more effective at low speeds. This increase in the maximum lift coefficient and reduction in stall speed reduces the wing area, providing greater efficiency in cruise. Some studies have indicated that propeller slipstream could increase the maximum lift coefficient as well as the angle of attack where stall occurs and, at the same time, decrease the loss of lift at angles of attack above stall, showing a much greater lift increase than is possible with conventional high lift devices. A near-uniform axial velocity can be produced aft of the propeller in order to increase the axial velocity and improve the high-lift capability (Patterson & German, 2015). Therefore, the application of distributed electric propulsion can increase the cruise efficiency reducing the necessary wing area during the low-speed flight phases. One popular example is the NASA X-57 Maxwell aircraft, which is based on a Tecnam P2006T aircraft fuselage and reconfigured with a much smaller wing than the baseline aircraft. The smaller wing is achievable for this design due to the high lift provided by 12 small electric propellers along the leading edge of the wing during the take-off and landing phases of flight (Borer, 2016). The aerodynamic interaction between the propeller slipstream and the lifting surface can be used to increase the lift coefficient and reduce the necessary wing surface in those phases requiring high lift values (e.g., take-off and landing). A model capable to consider these effects from the early stages is briefly described here. For the present work, the effects of the lifting surface on the propeller efficiency due to the upwash is not considered. The interaction between the propeller slipstream and the lifting surface, on which the propulsive system is mounted, depends on the geometry of the two elements.

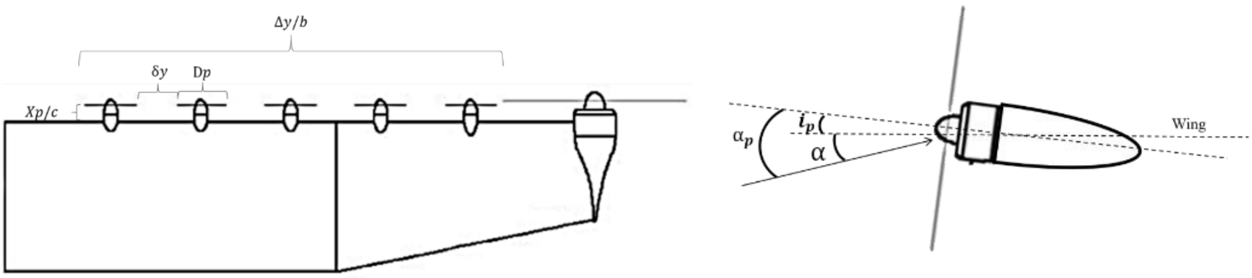

Figure 29. Distributed electric propulsion geometry.

The system is characterized by N propellers ($N/2$ propellers per semi-span) of diameter D_p (R_p is the radius). As shown in Figure 29, three geometrical parameters represent the position and the distribution of the propulsive system and the propeller disks: the parameter $\Delta y/b$ represents the wingspan fraction occupied by distributed propulsion, δy is the gap between the propellers in percentage of propeller disk diameter, and x_p/c is the axial position of the propeller disk from the leading edge in unit chord. The thrust line of secondary propulsors is at an angle α_p with respect to freestream velocity. The angle i_p between the propeller disk axis and the wing chord represents the incidence of the propeller. Finally, the angle between the wing chord and the freestream velocity is the angle of attack α. T_p is the total thrust produced by distributed propellers. The actuator disk theory drives the estimation of the axial induction factor, representing the percentage increase in speed evaluated at propeller disk's location:

$$a_p = \frac{1}{2}\left(\sqrt{1 + \frac{8}{\rho\,\pi\,V^2}\frac{T_p}{D_p^2}} - 1\right) \qquad \textbf{(4)}$$

The induced velocity at the propeller disk's location is implied by Eq. (4):

$$w_p = a_p V_\infty \tag{5}$$

Considering the *contraction ratio* of the slipstream evaluated at ¼ of the local chord:

$$\frac{R_{c/4}}{R_p} = \sqrt{\frac{1 + a_p}{1 + a_p\left(1 + X_{p_{c/4}} \Big/ \sqrt{{X_{p_{c/4}}}^2 + {R_p}^2}\right)}} \tag{6}$$

A CFD-based *finite-slipstream correction factor*, *β*, is necessary when $R_{c/4}$ is little compared to the airfoil chord. Finally, the bidimensional lift coefficient increase due to aero propulsive interactions is estimated by the following equation:

$$\Delta c_l = 2\pi \left[\left(\sin\alpha - a_{c/4}\beta \sin i_p\right)\sqrt{(a_{c/4}\beta)^2 + 2a_{c/4}\beta\cos\left(\alpha + i_p\right) + 1} - \sin\alpha\right] \tag{7}$$

The bidimensional drag coefficient variation is estimated by the sum of two different contribution, i.e., the *induced drag* coefficient variation and the *skin friction* contribution:

$$\Delta C_{d0} = a_{c/4}^2\, c_f \tag{8}$$

$$\Delta C_{di} \simeq \frac{2C_l \Delta C_l}{\pi AR} \tag{9}$$

In Equation (8), c_f is the skin friction coefficient, and C_l is the total lift coefficient in Eq. (9). Corresponding three-dimensional coefficients are defined by multiplying the above bidimensional coefficients by $\Delta y/b$, that is the ratio of wingspan covered by the slipstream of distributed propellers.

Some results are shown in Table 10 to give a better impression of the entity of DEPs' effect on wing aerodynamic coefficients. Results are relative to a case with 62% coverage by distributed propellers, rotating at 3000 RPM and producing 60000 N of total thrust. Considered flight speed was 60 m/s, and the wing had an aspect ratio, *AR*, equal to 15.0.

Table 10. Effect of distributed electric propulsion on lift and drag coefficients.

Number of DEPs	Take-Off Conditions (Clean C_L = 2.10)			Landing Conditions (Clean C_L = 2.70)		
	ΔC_L	ΔC_{Di}	ΔC_{D0}	ΔC_L	ΔC_{Di}	ΔC_{D0}
8	0.7427	0.0661	0.0003	0.9141	0.1047	0.0003
12	0.9758	0.0869	0.0008	1.2047	0.1379	0.0008
16	1.1168	0.0994	0.0014	1.3810	0.1581	0.0014
20	1.2083	0.1076	0.0022	1.4957	0.1712	0.0022

4.5. Tip-mounted propeller

Previous wind tunnel tests and analytical and computational modeling have indicated that using wingtip mounted propellers can have significant performance benefits. By placing the propellers in front of the wings on the tips, the rotation of the propellers can be used to counter the effects of the wingtip vortices to effectively push them further outward, which can reduce induced drag. The potential also exists to use propellers and electric motors at the wingtips as turbines to extract energy from the tip vortices. Furthermore, since electric motors can also be operated in "reverse" as generators to extract power, no additional mass would be required to enable some battery recharge capability.

In general, the induced drag can be approximated accordingly to Eq. (7) and Eq. (9), but the effect due to the swirl in propeller slipstream would be neglected. As shown in Figure 30, the presence of the wing causes a decrease in the angle of attack related to the induced downwash speed, w_w. The induced angle of attack due to the wing, also called *downwash angle*, α_{iw}, linearly increases with lift coefficient.

The variation of the axial speed causes an upwash effect counteracting the downwash due to the wing. Finally, the flow rotation due to the propeller slipstream must be also accounted. Assuming a certain rotation direction of the propeller, the tangential induction is a measure of the ratio between the propeller angular speed, **Ω**, and the angular speed induced on the flow downstream of the propeller, ω, and it can be used to estimate the vertical speed due to the slipstream. The tangential induction due to propeller can be computed through Eq. (11):

$$a_{p_t} = \frac{\omega}{2\Omega} = \frac{1}{2} - \sqrt{\frac{1}{4} - \frac{V^2}{\Omega^2 R_p^2}(1 + a_p)a_p} \quad \textbf{(10)}$$

The tangential speed perceived in the propeller slipstream, w_{swirl}, is a function of the tangential induction, the tangential speed of the tip of the propeller and the propeller radius, and it can be computed through Eq. (11):

$$w_{\text{swirl}} = a_{p_t} \Omega R_p \quad \textbf{(11)}$$

Finally, the induced angle can be computed accordingly to Eq. (11):

$$\alpha_{ip} = \tan^{-1}\left(\frac{w_w + w_p + w_{swirl}}{V_\infty + w_P}\right) \quad \textbf{(12)}$$

It is clearly understandable that, properly rotating the tip propeller in the opposite direction respect to the tip-vortex (inner-up direction), it is possible to reduce the induced angle of attack and so the induced drag. Numerical and experimental analysis clearly confirm the induced drag reduction due to the tip propeller. Combining the effect of the wing and of the propeller (see also Figure 30), the variation of the induced drag coefficient can be expressed as reported in the following equation, where α_{ip} is the angle induced by the propeller and α_{iw} is the one for which the wing is responsible:

$$\Delta C_D = -\frac{\Delta y/b}{N-1}\frac{C_L^2}{\pi A R e} + \frac{\Delta y/b}{N-1}\left(\frac{V_p}{V}\right)^2 C_{L_\alpha}(\alpha - \alpha_{ip})(\alpha_{iw} - \alpha_{ip}) \quad \textbf{(13)}$$

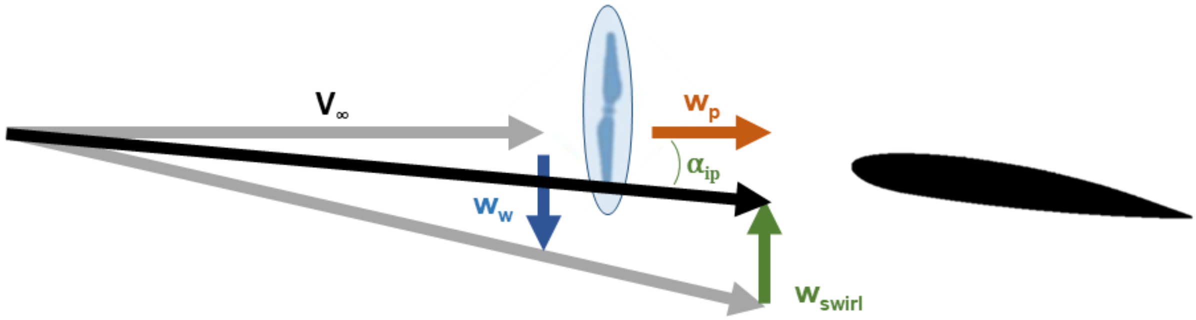

Figure 30. Induced angle due to wing and rotating disk.

5. GENESIS hybrid propulsion system synthesis

5.1. Preliminary application of the aircraft design chain

The aero-propulsive effects investigated in Sec. 4 have been included into a design chain which combines the aircraft conceptual design activity and the analysis of mission energy requirements into a comprehensive multi-disciplinary approach, summarized in Figure 31. The conceptual design aims to choose a single aircraft configuration, which suits the TLAR and aviation regulations requirements. In case of a hybrid-electric aircraft, it is important to explore different powertrain operating modes with the mission profile to maximize the efficiency of the air transport.

Such investigation may be included in an optimization loop targeting, for instance, minimum weight penalties, reduced emissions, and minimized DOC. The conceptual design workflow is divided in three main modules. The **preliminary design** process moves from the statistical definition of the main geometrical characteristics depending on top-level requirements. It is a necessary step to have a baseline when designing a completely new aircraft. The following step is the **sizing** phase, which starts after fixing the characteristics of the propulsive architecture in terms of geometry, hybridization parameters, and operating modes. The evaluation of aviation regulation constraints and mission requirements yield to the choice of the *sizing point*, that is the combination of wing loading *W/S* and weight-to-power *W/P*. The last step is the **analysis** of the energetic requirements and flight performance, which is a crucial step to verify the compliance with aviation regulations and TLAR, and to optimize the aircraft.

The reason why this section was started with the introduction of the design chain under development at the University of Naples "Federico II" is that it was used to provide a preliminary estimate of the energy requirement for a typical mission. All methods have been implemented in a MATLAB based software constituting a state-of-the-art conceptual design, analysis and optimization toolchain for conventional and hybrid-electric powerplant architectures. Depending on the hybridization strategy chosen, this requirement can be met by means of different energy sources, such as batteries, hydrogen, biofuels or conventional aviation fuel.

Distributed electric propulsion (DEP) has been identified as the most promising innovative technology, more suited to the short-term time horizon. In fact, it fits perfectly with the use of batteries as secondary energy sources, supporting the burnt fuel, in a way similar to that shown in Figure 24. As demonstrated by the example of the NASA X-57 Maxwell, this technology is in fact already mature, and the next logical step is to verify the advantages of an application on regional 50-seat aircraft. In the case of the GENESIS project, the serial/parallel partial hybrid electric powertrain seems to be the most promising in terms of flexibility and global efficiency for the configuration considered.

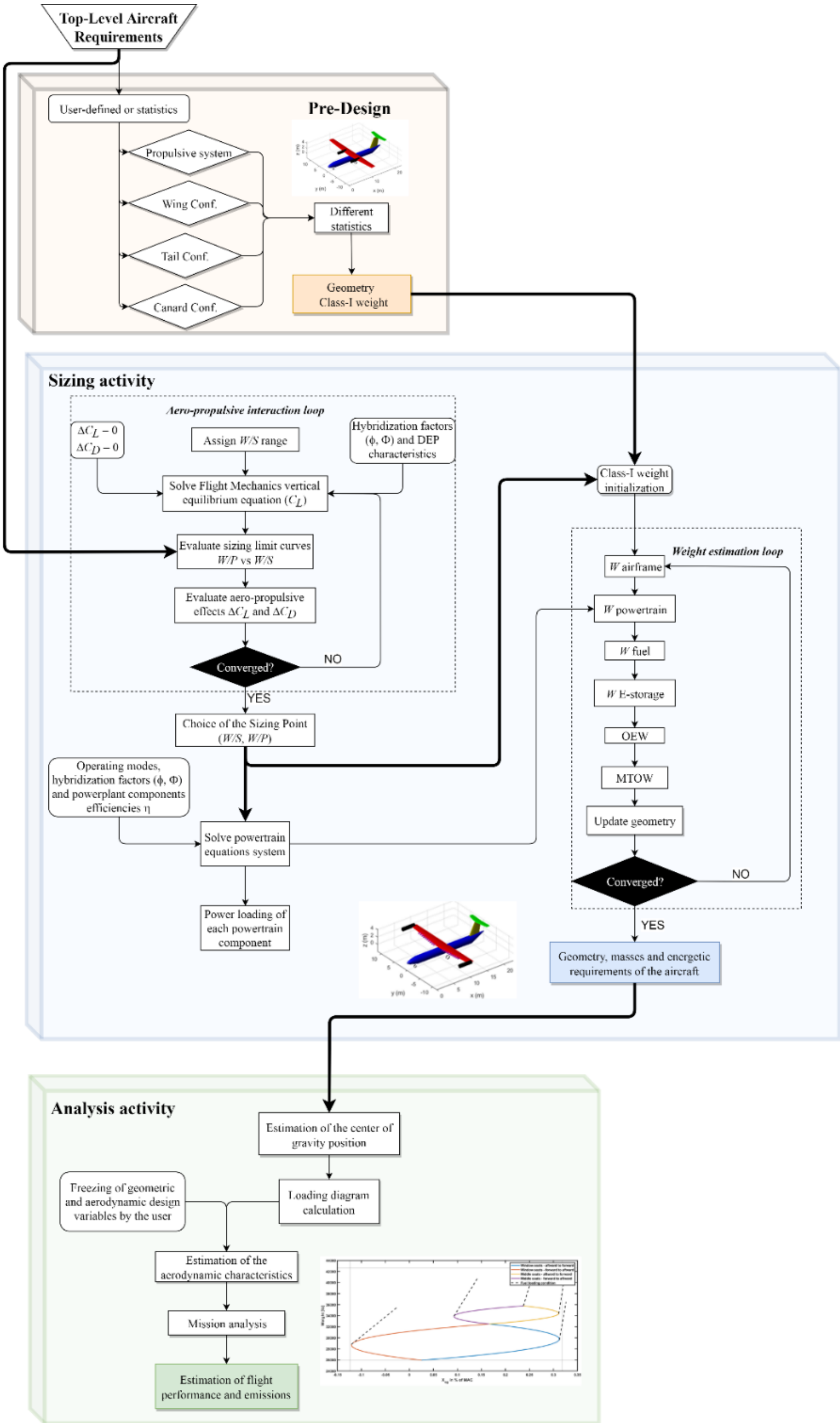

Figure 31. Design chain workflow.

The use of *synfuels*, not involving a drastic change in today's conception of aeronautical propulsion, also represents a valid alternative to investigate for the short-term time horizon, aiming for an expected reduction of emissions between 30% and 60%. In fact, regarding refueling and on-ground handling, one of the biggest problems to consider is that handling a new fuel will also call for new safety regulations, which could potentially inhibit parallel operations. However, unlike hydrogen, today's airport infrastructure may already be ready to handle synfuels as it is comparable to kerosene and today's aircraft operations. Furthermore, the serious safety and thermal management problems induced by the use of hydrogen require parallel work by the regulatory authorities, which must update the certification rules in order to guarantee the airworthiness of this new category of aircraft. This scenario is not likely to be realized within the next decade. In fact, specific powers **above 2 kW/kg** have been identified as the minimum requirement to make the use of fuel cells competitive in aviation, and aircraft equipped with similar systems are expected to become commercial not earlier than 15 years (Figure 32). For these reasons, UNINA identifies fuel cells as the main propulsive technology to bet on for medium-term and long-term scenarios, given the potential of hydrogen propulsion to reduce climate impact by up to 90% (Clean Sky 2 and European Commission, 2020). However, a value of **4 kW/kg** would be optimal for the fuel cell system to facilitate the transition from a traditional to a hydrogen-based configuration. Even for configurations based on hydrogen, the use of electric motors distributed along the wing can be useful to aim for high-efficient wings, but it is important to quantify the real gain of such a complication in terms of weight, already highly penalized as a result of the LH2 tanks and fuel cell systems, as well as analyzing the acquisition and maintenance costs.

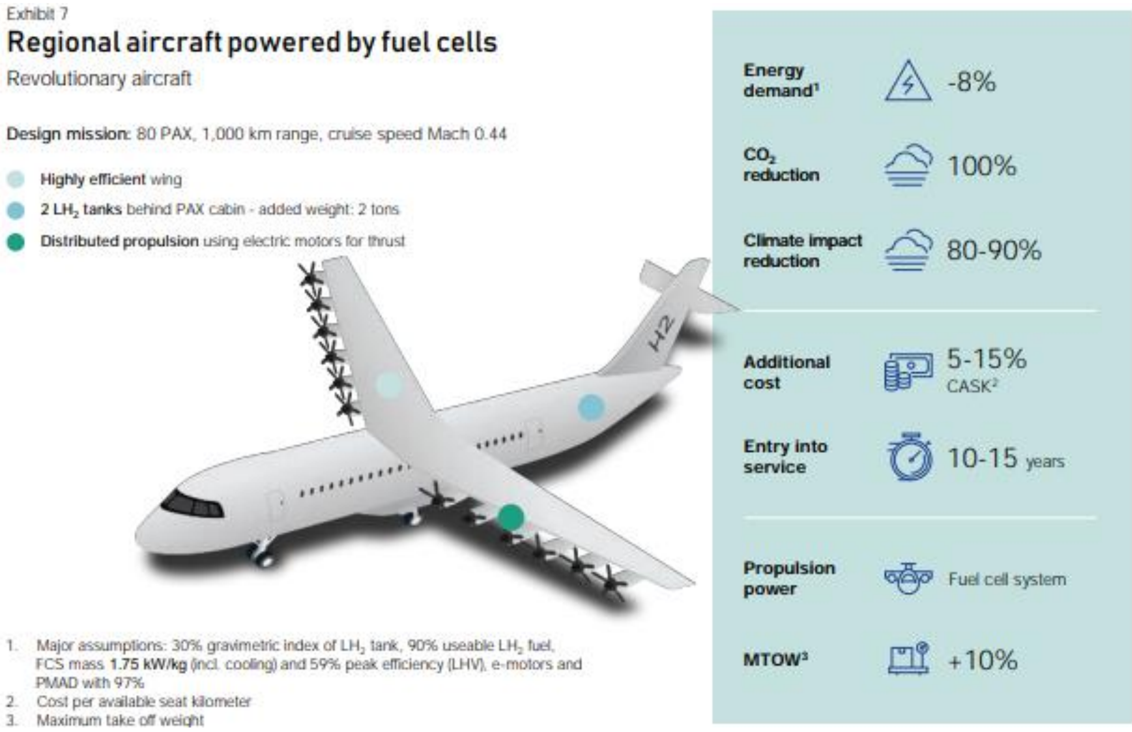

Figure 32. Economic and climate impact of a revolutionary regional aircraft **(Clean Sky 2 and European Commission, 2020)**.

On the contrary, the switch to hydrogen requires a redesign to incorporate large, heavy LH_2 tanks. More in general, systems based on fuel cells, especially if powered by hydrogen, have to deal with problems related to the penalizing weight increase of the aircraft, which affects its performance.

An accurate weight estimate is necessary in order to properly take these aspects into account, starting with the structural masses with particular reference to the wing, target of the optimization discussed above. In this sense, the methods being developed by TU Delft will be usefully integrated into the design chain to refine the estimation of the operating empty weight, the starting point for a refined analysis of the mission energy requirement. In this preliminary phase of the project, however, a semi-empirical method was used for the estimation of the weights (Torenbeek, 1982), and a hybrid-electric architecture with two thermal engines, two battery packs and 8 DEPs was used to benefit from the aero-propulsive effects exclusively during the take-off, climb and landing phases. This choice was guided by the results of previous investigations and the desire to limit the number of engines for reasons of weight, cost and additional aerodynamic drag, while ensuring full coverage of the wing. Two tip propellers were installed at the wingtips to mitigate the drag increase. However, an overview of the entire flight mission is given in Figure 33.

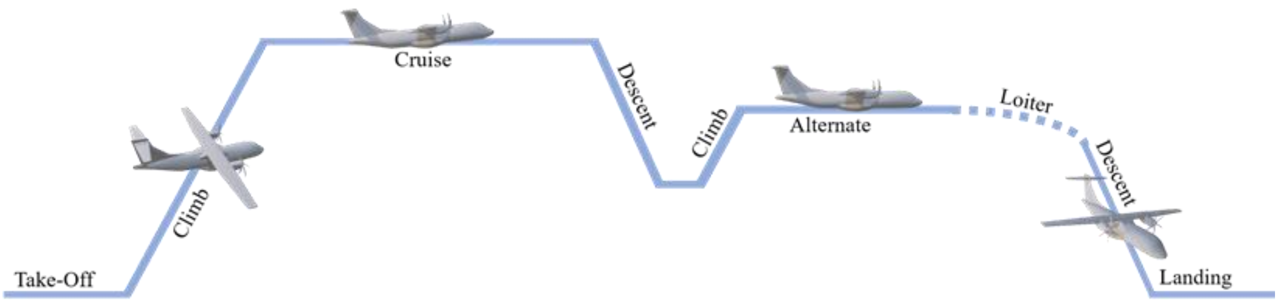

Figure 33. Design Mission.

A shaft power ratio equal to 0.8 in take-off, and equal to 0.5 in climb and landing, has been assumed for the year 2035 configuration. During cruise and along the routes to alternate airports, no use of the secondary propulsion was foreseen. The aircraft has been provided with 3 tons of battery with specific energy of 350 Wh/kg and specific power equal to 1 kW/kg. These hypotheses have been considered realistic for a medium-long term scenario, but in any case sufficiently reliable for a first estimate of the energy requirement. A refinement of the assumed technological level will follow the interaction with the WP2 partners planned for the near future. The estimated energy for the hypothesized mission amounts to about 6.8 MWh, corresponding to a certain mass of fuel depending on the degree of hybridization chosen. A specific energy of 12 kWh/kg was assumed for hydro-carbon fuel, and 33 kWh/kg for hydrogen. The efficiency of thermal engines was around 30% in all phases. Battery's supplied power ratio has been set to 12% at take-off in order to slightly downsize the gas turbines. The rest of the battery's energy is used during the cruise to reduce fuel consumption. The preliminary analysis carried out can form the basis for a preliminary estimate of the LH_2 requirement in the case of a partial or total replacement of kerosene. Table 11 reports the energy requirements from the three energy sources and provides a rough indication of the mass of hydrogen involved for four different levels of hydrogen usage. Reported percentages refer to the net output power, which means that the corresponding system's efficiency has already been considered. A similar procedure has been used to produce the energy breakdown for a year 2050 configuration (Table 12), provided 4.3 tons of battery with a specific energy density of 500 Wh/kg and a specific power of 1 kW/kg. The analyses must be considered absolutely not detailed, since real consumption cannot ignore the masses induced by the use of hydrogen and the technological level chosen for fuel cells. Different assumptions have been made about aerodynamics and the efficiency of each powerplant component, depending on the time horizon and based on UNINA's experience. The increase in mass would lead to greater aerodynamic drag and therefore to higher consumption, making the whole process iterative. Nevertheless, the estimated masses can constitute points of interest for the evaluation of the masses of the tanks and of the other collateral masses induced by cryogenic hydrogen. The development of a model for the estimation of hydrogen tanks will be the subject of the next phases of the project, thanks also to the outputs of WP2.2.

Table 11. Shaft power ratios and hydrogen consumption for different mission strategies (year 2035). Efficiency of fuel cell system has been assumed to be 60%. Total required energy is 6.8 MWh.

Flight Phase	Shaft Power Ratio	Battery Energy [%]	Fuel Energy [%]	LH2 Energy [%]	LH_2 Mass [kg]
Strategy 1					
Take-Off	0.8	31.1	37.7	31.2	0.5
Take-Off 2 Climb	0.5	16.5	67.0	16.5	4.1
Climb	0.5	22.5	55.0	22.5	5.8
Cruise	0.0	14.9	70.2	14.9	30.8
Descent	0.0	0.0	100.0	0.0	0.0
Climb 2 Alternate	0.0	0.0	100.0	0.0	0.0
Alternate	0.0	0.0	100.0	0.0	0.0
Descent from Alternate	0.0	0.0	100.0	0.0	0.0
Loiter	0.0	0.0	100.0	0.0	0.0
Descent 2 Landing	0.8	0.0	100.0	0.0	0.0
Landing	0.8	0.0	100.0	0.0	0.0
Total					**41.3**
Strategy 2					
Take-Off	0.8	31.1	8.9	60.0	1.1
Take-Off 2 Climb	0.5	16.5	48.5	35.0	8.6
Climb	0.5	22.5	29.5	48.0	12.5
Cruise	0.0	14.9	50.1	35.0	72.4
Descent	0.0	0.0	100.0	0.0	0.0
Climb 2 Alternate	0.0	0.0	100.0	0.0	0.0
Alternate	0.0	0.0	100.0	0.0	0.0
Descent from Alternate	0.0	0.0	100.0	0.0	0.0
Loiter	0.0	0.0	100.0	0.0	0.0
Descent 2 Landing	0.8	0.0	100.0	0.0	0.0
Landing	0.8	0.0	100.0	0.0	0.0
Total					**94.5**
Strategy 3					
Take-Off	0.8	31.1	0.0	68.9	1.2
Take-Off 2 Climb	0.5	16.5	41.8	41.7	10.2
Climb	0.5	22.5	17.5	60.0	15.6
Cruise	0.0	14.9	15.1	70.0	144.8
Descent	0.0	0.0	100.0	0.0	0.0
Climb 2 Alternate	0.0	0.0	100.0	0.0	0.0
Alternate	0.0	0.0	50.0	50.0	13.2
Descent from Alternate	0.0	0.0	100.0	0.0	0.0
Loiter	0.0	0.0	100.0	0.0	0.0
Descent 2 Landing	0.8	0.0	100.0	0.0	0.0
Landing	0.8	0.0	100.0	0.0	0.0
Total					**185.0**
Strategy 4					
Take-Off	0.8	31.1	0.0	68.9	1.2
Take-Off 2 Climb	0.5	16.5	0.0	83.5	20.5
Climb	0.5	22.5	0.0	77.5	20.1
Cruise	0.0	14.9	0.0	85.1	176.0
Descent	0.0	0.0	0.0	100.0	3.0
Climb 2 Alternate	0.0	0.0	0.0	100.0	17.7
Alternate	0.0	0.0	0.0	100.0	26.3
Descent from Alternate	0.0	0.0	0.0	100.0	2.1
Loiter	0.0	0.0	0.0	100.0	37.0
Descent 2 Landing	0.8	0.0	0.0	100.0	0.4
Landing	0.8	0.0	0.0	100.0	0.0
Total					**304.3**

Table 12. Shaft power ratios and hydrogen consumption for different mission strategies (year 2050). Efficiency of fuel cell system has been assumed to be 60%. Total required energy is 5.5 MWh.

Flight Phase	Shaft Power Ratio	Battery Energy [%]	Fuel Energy [%]	LH_2 Energy [%]	LH_2 Mass [kg]
Strategy 1					
Take-Off	0.9	59.1	20.3	20.6	0.4
Take-Off 2 Climb	0.5	47.5	0.0	52.5	7.3
Climb	0.5	57.7	21.7	20.6	6.3
Cruise	0.0	2.5	80.0	17.5	27.0
Descent	0.0	0.0	100.0	0.0	0.0
Climb 2 Alternate	0.0	0.0	100.0	0.0	0.0
Alternate	0.0	0.0	100.0	0.0	0.0
Descent from Alternate	0.0	0.0	100.0	0.0	0.0
Loiter	0.0	0.0	100.0	0.0	0.0
Descent 2 Landing	0.0	0.0	100.0	0.0	0.0
Landing	0.5	0.0	100.0	0.0	0.0
Total					**41.0**
Strategy 2					
Take-Off	0.9	59.1	0.0	40.9	0.7
Take-Off 2 Climb	0.5	47.5	0.0	52.5	7.3
Climb	0.5	57.7	0.0	42.3	12.8
Cruise	0.0	2.5	50.0	47.5	73.3
Descent	0.0	0.0	100.0	0.0	0.0
Climb 2 Alternate	0.0	0.0	100.0	0.0	0.0
Alternate	0.0	0.0	50.0	50.0	9.8
Descent from Alternate	0.0	0.0	100.0	0.0	0.0
Loiter	0.0	0.0	100.0	0.0	0.0
Descent 2 Landing	0.0	0.0	100.0	0.0	0.0
Landing	0.5	0.0	100.0	0.0	0.0
Total					**104.0**
Strategy 3					
Take-Off	0.9	59.1	0.0	40.9	0.7
Take-Off 2 Climb	0.5	47.5	0.0	52.5	7.3
Climb	0.5	57.7	0.0	42.3	12.8
Cruise	0.0	2.5	0.0	97.5	150.5
Descent	0.0	0.0	0.0	100.0	2.3
Climb 2 Alternate	0.0	0.0	0.0	100.0	19.0
Alternate	0.0	0.0	0.0	100.0	19.6
Descent from Alternate	0.0	0.0	0.0	100.0	1.1
Loiter	0.0	0.0	0.0	100.0	35.1
Descent 2 Landing	0.0	0.0	0.0	100.0	0.1
Landing	0.5	0.0	0.0	100.0	0.0
Total					**248.6**

The real optimal degree of hybridization, and therefore the quantity of hydrogen required, cannot be determined from the early stages of the project. This is related to the fact that it is not possible to predict the impact of induced masses on total energy consumption, and in general much more in-depth analyses are necessary. Nevertheless, these preliminary calculations have allowed the identification of some specification points in terms of mass of hydrogen which hopefully explore the entire range of possible masses required. The design of the tanks and the evaluation of all the induced masses will allow UNINA to generate a surrogate model to be included in its design chain for the final assessment. Since the presented results are based on constant maximum take-off mass, by virtue of the mass increase linked to the power density of fuel cells lower than thermal systems, UNINA suggests using mass values of hydrogen increased by 50% for the first design loop of the tanks with respect to the values specified in Table 11 and Table 12. The additional mass would be useful to increase the operational flexibility of the aircraft. Finally, the specification points for the three preliminary configurations are reported in Table 13, referring to the short-term, medium-term and long-term time horizons. They were obtained on the basis of the technological level of the battery reported in Table 7, simulating the power requirements for each phase of the mission. The shaft power ratios for the short-term configuration are the same as previously mentioned for the medium-term configuration, and therefore reported in Table 11. These maximum powers required are all related to the take-off phase. To compensate for the optimistic assumption about technology level, a safety margin was assumed, and battery usage limited during the design mission. Again, due to the unpredicted mass penalties, a further safety margin for the first design loop of 20% is suggested in order to be conservative.

Table 13. Power specification points for the three time horizons.

Powertrain Component	Number	Reference Power [kW]		
		Year 2025-2035	Year 2035-2050	Year 2050+
Gas turbine	2	2400	0	0
Fuel cell system	2	0	1800	1400
Battery pack	2	550	1100	2000
Primary electric machine	2	1200	1200	100
Secondary electric machine	8	600	600	750

6. References

A. ATAG Air Transport Action Group. (2021, 07 10). *ATAG* . Retrieved from https://www.atag.org/facts-figures.html

B. ATR. (2018). *Turboprop market forecast.*

C. AviationPros. (2020, 09). *Airbus Reveals New Zero-Emission Concept Aircraft.* Retrieved from https://www.aviationpros.com/

D. Boeing. (2021, 07 02). *Boeing commercial maket*.

E. Boeing. (n.d.). *Boeing Environmental Report 2020.*

F. Borer, N. P. (2016). Design and Performance of the NASA SCEPTOR Distributed Electric Propulsion Flight Demonstrator. *16th AIAA Aviation Technology, Integration, and Operations Conference.*

G. Ciliberti, D., Orefice, F., Della Vecchia, P., Nicolosi, F., & Corcione, S. (2019). An Approach To Preliminary Sizing of Turbo-Electric Aircraft With Distributed Propulsion. *AIDAA XXV International Congress.*

H. Clean Sky 2. (2021, 06). *Regional Aircraft Opportunities*. Retrieved from https://www.cleansky.eu/regional-aircraft
I. Clean Sky 2 and European Commission. (2020). *Hydrogen-powered aviation.*
J. de Vries, R., Brown, M. T., & Vos, R. (2018). A Preliminary Sizing Method for Hybrid-Electric Aircraft Including Aero-Propulsive Interaction Effects. *2018 Aviation Technology, Integration, and Operations Conference.*
K. de Vries, R., Brown, M., & Vos, R. (2018). A Preliminary Sizing Method for Hybrid-Electric Aircraft.
L. Felder, J. L. (2015). NASA Electric Propulsion System Studies. *NASA Presentation.*
M. German, B., Bradley, M., McDonald, R., & Vos, R. (2018). Design of Electric and Hybrid-Electric Aircraft. *AIAA Aviation Conference*.
N. Gleave, S. (2004). Adapted from Commission for Integrated Transport.
O. Graver, B., Zhang, K., & Rutherford, D. (2019, 09). CO2 emissions from commercial aviation, 2018.
P. *https://ourairports.com/*. (2021, 07). Retrieved from https://ourairports.com/
Q. ICCT - The International Council of Clean Transportation. (2020). CO2 EMISSIONS FROM COMMERCIAL AVIATION.
R. Michaelides, E. E. (2012). *Alternative Energy Sources.* Springer.
S. Orefice, F., Della Vecchia, P., Ciliberti, D., & Nicolosi, F. (2019). Aircraft Conceptual Design Including Powertrain System Architecture and Distributed Propulsion. American Institute of Aeronautics and Astronautics (AIAA).
T. OurWorldinData.org – Research and data to make progress against the world's largest problems. (2021, 04 20). *OUR WORLD IN DATA*. Retrieved from https://ourworldindata.org/
U. Patterson, M. D., & German, B. J. (2015). Simplified Aerodynamics Models to Predict the Effects of Upstream Propellers on Wing Lift. *53rd AIAA Aerospace Sciences Meeting.*
V. Statista.com. (2021, 04 02). Retrieved from https://www.statista.com/
W. Strack, M., Pinho Chiozzotto, G., Iwanizki, M., Plohr, M., & Kuhn, M. (2017). Conceptual Design Assessment of Advanced Hybrid Electric Turboprop Aircraft Configurations. *17th AIAA Aviation Technology, Integration, and Operations Conference.*
X. The National Academies of Sciences, Engineering and Medicine. (2016). *Commercial Aircraft Propulsion and Energy Systems Research.* The National Academies Press.
Y. Torenbeek, E. (1982). *Synthesis of Subsonic Airplane Design: An Introduction to the Preliminary Design, of Subsonic General Aviation and Transport Aircraft, with Emphasis on Layout, Aerodynamic Design, Propulsion, and Performance.* Delft University Press.
Z. Trading Economics . (2021, 07 20). Retrieved from https://tradingeconomics.com/commodity/crude-oil
AA. Zamboni, J. (2018). *A Method for the Conceptual Design of Hybrid Electric Aircraft.* Delft University of Technology.